the stabilization of p53.[19] However, although Arf is a nucleolar protein that binds and inactivates MDM2 in the nucleoplasm, Korgaonkar *et al.* showed that Arf functions primarily outside the nucleolus, and it is sequestered and held inactive in the compartment by NPM.[28] Most likely, NPM inhibits Arf's p53-dependent activity by targeting it to nucleoli and impairing ARF–MDM2 association.

In accordance with these findings, knock-out (KO) mice of the *NPM1* gene show mid-stage embryonic lethality due to the accumulation of DNA damage, activation of p53, and widespread apoptosis.[29,30] Double KO mice of *TP53* and *NPM1* rescue apoptosis *in vivo* and fibroblast proliferation *in vitro*.[29] In the absence of NPM, Arf protein is excluded from nucleoli and is markedly less stable. It has been suggested that NPM regulates DNA integrity through Arf–MDM2–p53.

Conversely, it was also shown that Arf inhibits the production of rRNA, retarding the processing of 47/45S and 32S precursors.[31] Itahana *et al.* further reported that Arf promotes polyubiquitination and degradation of NPM.[32] Accordingly, there is a molecular association between NPM and Arf, which implies a new role for the nucleolus in oncogenesis.

NPM–ALK chimeric kinase in ALCL

Anaplastic large cell lymphoma is a T-cell lymphoma that is characterized by abundant cytoplasm, pleomorphic nuclei and CD30 expression.[33] ALCL accounts for approximately 3% of adult non-Hodgkin's lymphoma and 10–30% of childhood lymphoma. Cytogenetically, the 2p23 locus is translocated frequently with 5q35, and less frequently with 1p25, 3q21 or 2q35.[34] In 1994, Morris *et al.* showed that the t(2;5) translocation fused the *NPM1* gene on 5q35 to a previously unidentified protein tyrosine kinase gene, *ALK*, on 2p23.[35]

In the NPM–ALK chimeric kinase, the N-terminus of NPM (amino acids 1–117) is fused to the catalytic domain of ALK (amino acids 1058–1620). Because its expression is regulated by the *NPM1* promoter, the fusion protein is expressed ectopically in lymphoid tissue. Wild-type ALK is a receptor tyrosine kinase that is expressed in the brain, spinal cord, small intestine and testis, but not in lymphoid cells. ALK belongs to the insulin receptor subfamily, although the natural ligand remains unclear.[36] In NPM–ALK, the N-terminal NPM domain is associated with oligomerization (Fig. 3) and causes constitutive activation of the ALK kinase. This mechanism is similar to that of BCR–ABL. NPM–ALK can associate with several adaptor proteins such as SHC, Grb2 and IRS-1, and is associated with the activated RAS–MAPK, PLCg, PI3K–Akt and JAK–STAT pathways.[34,37–39] Experiments using Ba/F3 cells revealed that NPM–ALK abrogates the interleukin-3 dependency of the cells and mediates signals for proliferation and survival.

Because NPM–ALK$^+$ lymphomas express CD30, a transmembrane receptor for CD30L, it has been asked whether CD30 and NPM–ALK are connected functionally.[40] In Hodgkin's lymphoma, overexpressed CD30 molecules aggregate on the cell surface ligand-independently, and form a TRAF–IKK–IKBα complex, which leads to nuclear factor kappa-B (NF-κB) activation.[41] In contrast, Horie *et al.* clarified that NPM–ALK disrupts CD30 signaling and constitutive NF-κB activation in ALCL.[42] TRAF2/5 was shown to be bound with NPM–ALK on both the kinase domain of ALK and the N-terminal domain of NPM. In the same study, wild-type NPM was shown to be tyrosine-phosphorylated by NPM–ALK, although the significance remains unclear.

Studies of subcellular localization of NPM and its chimeric proteins reveal another aspect of the oncogenic role of NPM.[43] As shown in Fig. 1, NPM–ALK consists structurally of the oligomerization and metal-binding domains of NPM together with an almost full-sized intracytoplasmic domain of ALK. It lacks the two nuclear localization domains and Asp/Glu-rich domains

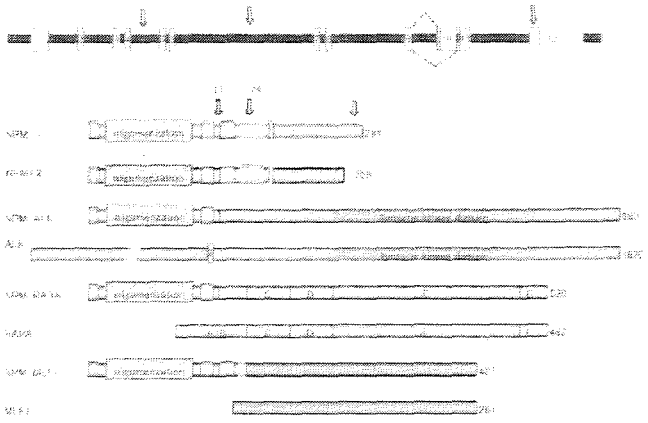

Fig. 1. The *NPM1* gene and its related cDNA. Two isoforms of *NPM1* cDNA differ at the C-terminus. Exon 9 is spliced with exon 11 in *NPM1.1*, whereas in *NPM1.2* it is spliced with exon 10 and the coding sequence is terminated prematurely. In nucleophosmin (NPM)–ALK, the cytoplasmic domain of ALK is fused with the N-terminal NPM domain, which contains an oligomerization domain. Similar to NPM–ALK, the entire functional domain of RARA is fused to the N-terminal NPM domain, which accelerates oligomerization and inactivation of retinoic acid-responsive transcription. Break points are indicated by yellow arrows. The clustering regions of mutations of exon 12 are indicated by a red arrow.

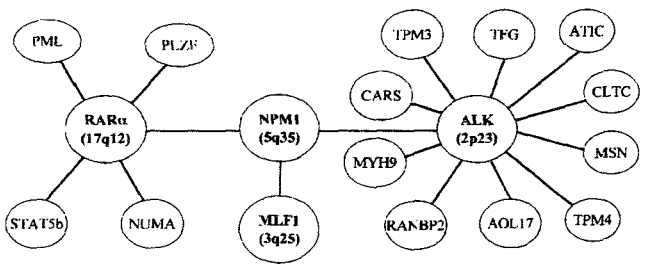

Fig. 2. Fusion genes with the *NPM1* gene.

of NPM. Accordingly, NPM–ALK is thought to be localized to the cytoplasm instead of nucleoli. Immunohistochemistry using anti-ALK stains both the nucleus and cytoplasm of ALCL cells[36,43,44] (Fig. 4). Anti-C-terminal NPM antibody is able to discriminate wild-type NPM from the fused protein. Interestingly, wild-type NPM is localized to the nucleus but not the cytoplasm, whereas NPM–ALK is distributed in both.

There are many *in vivo* studies on the oncogenic role of NPM–ALK.[39] Mice transplanted with bone marrow cells infected with retrovirus containing human *NPM1–ALK* cDNA developed B-cell lymphoma, not ALCL. However, in transgenic mice carrying *NPM1–ALK* cDNA under the control of the murine CD4 promoter or Moloney murine leukemia virus Long Terminal Repeat (LTR), T-cell tumors resembling human ALCL developed, suggesting that the phenotype depends on the promoter.

NPM–RARα chimeric transcription factor in APL

Acute promyelocytic leukemia is characterized by myeloid malignancies with a maturational block at the promyelocytic stage.[33] Treatment with all-*trans* retinoic acid (ATRA) overcomes this maturation arrest and induces differentiation of APL blasts.[45] APL is usually accompanied by t(15;17), which

doi: 10.1111/j.1349-7006.2006.00270.x

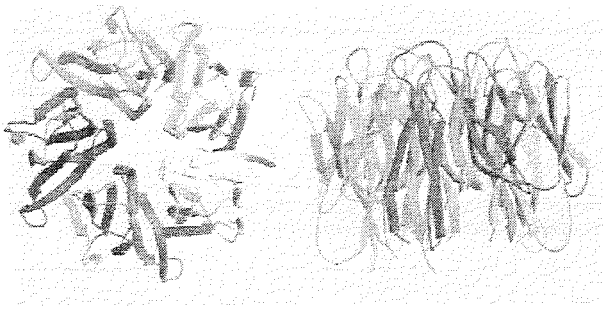

Fig. 3. The structure of the N-terminal domain of *Xenopus* nucleoplasmin (Np-core), which is related to NPM1, was reported by Namboodiri *et al.*[73] The Np-core monomer forms a barrel shape consisting of eight-stranded β-sheets, and the barrel forms a stable pentamer. Two pentamers further associate to form a decamer. The authors showed that both Np and Np-core are able to assemble large complexes that contain the four core histones. These complexes each contain five histone octamers that dock to a central Np decamer. Dutta *et al.* provided models of histone storage, sperm chromatin decondensation and nucleosome assembly.[15]

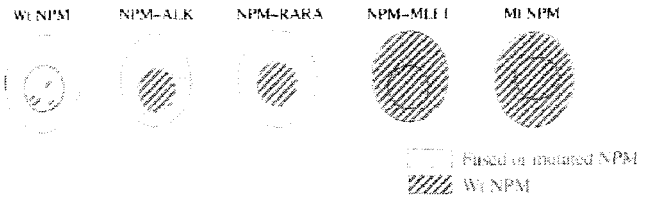

Fig. 4. Subcellular localization of nucleophosmin (NPM) and its fused proteins. The distribution of NPM–ALK homodimer is limited to the cytoplasm, but the nucleolar localization motifs present in wild-type (Wt) NPM permits entry of the NPM/NPM–anaplastic lymphoma kinase (ALK) heterodimers to the nucleus and nucleolus.[36] Although data of the localization of NPM–RARα is limited, transfection of *NPM1–RARA* into Hela cells showed a diffuse pattern of nuclear localization.[57] In contrast, NPM–MLF1 and wild-type NPM were stained by using anti-C-terminal NPM antibody.[60]

forms the *PML–RARA* fusion gene.[46] In addition, molecular variants of APL have been described in which *RARA* is fused to one of four other genes: *PLZF*, *NUMA*, *STAT5b* or *NPM1*.[46,47] Common features of all of these proteins are that the B through F regions of RARα, which contain its DNA and ligand-binding domains, have N-terminal non-RARα moieties that add dimerization ability to each fusion protein. Homodimerization or heterodimerization is thought to be associated with the repression of retinoid-responsive transcription and perhaps with other alterations in transcription.

The first APL case with a t(5;17) translocation was described in 1994 and the sequence of chromosomal joint was cloned in 1996.[48,49] This variant type of APL was clinically sensitive to ATRA, and the sensitivity was later confirmed *in vitro*.[50] The N-terminal NPM portion fuses with RARα in a similar manner to other APL fusion products. Like other APL fusion products, NPM–RARα forms a heterodimer with RXR or NPM. These dimers recruit corepressor complexes and repress retinoid-responsive transcription in a dominant-negative manner.[51] Homodimer formation of RARα may be a crucial event in APL pathogenesis *in vivo*.[52] In transgenic mice, NPM–RARα enhanced the proliferation of myeloid cells, mimicking myeloproliferative disease and, later, the transgenic mice developed an APL-like disease with blasts that were sensitive to ATRA.[53]

In the case of PML–RARα, immunostaining with anti-PML antibody revealed a microgranular pattern, which differs from the microspeckled one observed in the case of wild-type PML.[54] ATRA treatment restored the aberrant localization to a speckled pattern through degradation of PML–RARα.[55,56] This finding implies that NPM–RARα also acts in a dominant-negative manner relative to wild-type PML, and this effect is cancelled by ATRA. Anti-NPM (N-terminus) antibody stained the nucleus with a diffuse microgranular pattern, whereas PML localization was normal.[57] It is interesting but remains to be studied how NPM–RARα affects the function of wild-type NPM.

NPM–MLF1 chimeric protein in AML/MDS

Yoneda-Kato *et al.* reported that the t(3,5) (q25.1;q34) translocation associated with AML/MDS (most frequently with the M6 French–American–British [FAB]-type) produces a 5′-NPM-coding sequence fused in-frame to a new gene, which they named *MLF1*.[10] The *MLF1* gene encodes a 268-amino-acid polypeptide that has no homology to any previously characterized protein and does not have known functional motifs. Expression of *MLF1* mRNA is observed in testis, ovary, skeletal muscle, heart, kidney and colon, but not in normal hematopoietic cells.

The function of MLF1 protein remains unclear, but it inhibits erythropoietin-induced differentiation, cell-cycle exit and p27KIP1 accumulation.[58] Hanissian *et al.* identified an MLF1-interacting protein (MLF1IP) that associates specifically with MLF1. MLF1IP has nuclear localization signals, two nuclear receptor-binding motifs (LXXLL), two leucine zippers, two polypeptide enriched in proline, glutamine, serine and threonine (PEST) residues and several potential phosphorylation sites.[59] MLF1IP seems to have an important role in erythroid differentiation, and MLF1 seems to regulate MLF1IP function negatively.

Immunostaining studies have shown that MLF1 is localized mainly in the cytoplasm, whereas the NPM–MLF1 fusion protein is localized in the nucleus, especially the nucleolus[60] (Fig. 4). NPM is a nuclear protein and therefore the N-terminal portion that is fused to MLF1 may carry the nuclear targeting signal. Thus, both the ectopic expression and aberrant subcellular localization of MLF1 seem to be associated with the interruption of erythroid differentiation, which may be the reason that *MPL–MLF1* is found entirely in M6 FAB-type AML/MDS.

Frameshift mutation of NPM1 in AML

During an extensive study of the subcellular localization of NPM, Falini *et al.* found a correlation between the presence of cytoplasmic NPM and clinical and biological features in AML samples.[61] Cytoplasmic NPM was detected in 35.2% of 591 bone marrow specimens from patients with primary AML but not in 135 secondary AML specimens or in 980 hematopoietic or non-hematopoietic neoplasms other than AML. It was associated with a wide spectrum of morphological subtypes of the disease from M0 to M7 except M3. A normal karyotype and responsiveness to induction chemotherapy were also related to cytoplasmic NPM. There was a high frequency of internal tandem duplications of FLT3 (FLT3/ITD) and lack of CD34 and CD133 expression. AML with cytoplasmic NPM carried novel mutations in exon 12 of the *NPM1* gene. In the most common mutation, called type A, a 4-bp nucleotide (TCTG) is inserted at the position encoding the 288th amino acid residue, causing a frameshift of the downstream coding sequence (Table 1). As a result, the C-terminal amino acid residues, 286DLWQWRKSL-COOH, are changed to 286DLCLAVEEVSLRK-COOH. So far, a total of 29 variant sequence mutations have been reported in the *NPM1* genes of 1557 patients. All of the NPM mutant proteins lose at least one of W288 and W290, and share the same last five amino

Table 1. Representative mutations of *NPM1* in AML

Mutation	Sequence	Predicted amino-acid
Wild type (*NPM1.1*)	GAT CTC TGG CAG TGG AGG AAG TCT CTT **TAA** GAAAATAG	-DLWQWRKSL
Mutation A	GAT CTC TGT CTG GCA GTG GAG GAA GTC TCT TTA AGA AAA **TAG**	-DLCLAVEEVSLRK
Mutation B	GAT CTC TGC ATG GCA GTG GAG GAA GTC TCT TTA AGA AAA **TAG**	-DLCMAVEEVSLRK
Mutation D	GAT CTC TGC CTG GCA GTG GAG GAA GTC TCT TTA AGA AAA **TAG**	-DLCLAVEEVSLRK

The four inserted nucleotides are underlined. Stop codon is in bold. The nucleolar localization signal WXW in the wild-type sequence is substituted by LXXXVXXVXL, which corresponds to a nuclear export signal, shown in the predicted amino-acid column.

acid residues (VSLRK). Thus, despite the genetic heterogeneity, all of these *NPM1* gene mutations have the common feature of a frameshift mutation at the C-terminal region. Nakagawa *et al.* noticed that this frameshift not only loses the nucleolar localization signal (WXW) but also gains a nuclear export signal (NES) consisting of LXXXVXXVXL.[62] Falini *et al.* further confirmed that both alterations are crucial for NPM mutant export from the nucleus to the cytoplasm.[63]

Falini *et al.* found that cytoplasmic staining of NPM could define the *NPM1* mutation-positive AML cases that had a normal karyotype, *NPM1* gene mutations, and responsiveness to induction chemotherapy.[61] Grisendi and Pandolfi noted that NPM staining in cases of AML with aberrant cytoplasmic localization of the protein is mostly cytoplasmic, which suggests that the mutant NPM acts predominantly on the product of the remaining wild-type allele, causing its retention in the cytoplasm by heterodimerization[64] (Fig. 4).

Based on the above report, Suzuki *et al.* identified similar *NPM1* mutations, including four novel sequence variants, in 64 of 257 (24.9%) Japanese patients with *de novo* AML.[65] *NPM1* mutations were associated with normal karyotypes and with *FLT3* mutations, but not with other mutations. In 190 patients without the M3 FAB subtype who were treated using the protocol of the Japan Adult Leukemia Study Group, multivariate analyses showed that the *NPM1* mutation was a favorable factor for achieving complete remission but was associated with a high relapse rate. Importantly, sequential analysis using 39 paired samples obtained at diagnosis and relapse showed that *NPM1* mutations were lost at relapse in two of the 17 patients who had *NPM1* mutations at diagnosis. The loss of *NPM1* mutation at relapse suggests that it is not necessarily needed for maintenance of the disease.

Schnittger *et al.* screened 401 AML patients with normal karyotypes treated using the German AML Cooperative Group Protocol 99 for *NPM1* mutations.[66] *NPM1* mutations were detected in 212 (52.9%) of the 401 patients. Fourteen mutations, including eight new variants, were identified. *NPM1*-mutated cases were frequently associated with *FLT3* mutations but rarely associated with *MLL* tandem duplication, *NRAS*, *KIT* and *CEBPA* mutations. The *NPM1*-mutated group had a higher complete remission (CR) rate, a tendency of longer overall survival (OS), and significantly longer event-free survival (EFS).

Roel *et al.* examined *NPM1* mutation status in a cohort of 275 patients with AML by denaturing high-performance liquid chromatography.[67] *NPM1* mutations are less frequent in younger patients than in those aged over 35 years. *NPM1* mutations are positively correlated with AML with high white blood cell counts, normal karyotypes, and *FLT3/ITD*. *NPM1* mutations are correlated inversely with the occurrence of *CEBPA* and *NRAS* mutations. AML patients with *NPM1* mutations have a significantly better OS and EFS than those without *NPM1* mutations. Finally, in multivariate analysis, *NPM1* mutations have an independent favorable prognostic value with regard to OS, EFS and DFS.

In 300 patients entered into the AML Study Group trials, *NPM1* mutations were identified in 48% of the patients, including 12 novel sequence variants, all leading to a frameshift in the C-terminus of NPM.[68] AML patients with *NPM1* mutations in the absence of *FLT3/ITD* define a distinct molecular and prognostic subclass of young adult AML patients with normal cytogenetics.

In a larger study, the clinical significance of *NPM1* mutation was further suggested. One thousand four hundred and eighty-five patients with AML were examined for *NPM1* exon 12 mutations using fragment analysis.[69] A 4-bp insert was detected in 408/1485 patients (27.5%). Sequence analysis revealed known mutations (type A, B and D) as well as 13 novel alterations in 229 of the cases analyzed. *NPM1* mutations were more prevalent in patients with normal karyotype (324/709; 45.7%) than in those with karyotype abnormalities (58/686, 8.5%; $P < 0.0001$), and were significantly associated with several clinical parameters (high bone marrow blasts, high white blood cell and platelet counts, women). *NPM1* alterations were associated with *FLT3/ITD* mutations, even if the cases analyzed were restricted to patients with normal karyotype. Analysis of the clinical impact in four groups (*NPM1* and *FLT3/ITD* single mutants, double mutants, and wild-type for both) revealed that patients having only an *NPM1* mutation had significantly better overall and disease-free survival and a lower cumulative incidence of relapse. In conclusion, *NPM1*-mutations represent a common genetic abnormality in adult AML. If not associated with *FLT3/ITD* mutations, mutant *NPM1* appears to identify patients with favorable response to treatment.

In summary, the *NPM1* mutation[61,65–70] is observed in a high percentage of *de novo* AML, and is associated with normal karyotype, *FLT3/ITD* and better response to chemotherapy (Table 2). It remains controversial whether the presence of *NPM1* mutation indicates a good prognosis, but it is clear that it indicates a good prognosis in patients without *FLT3/ITD*. Structurally, a newly generated NES sequence at the C-terminus is a common feature, although more than 20 different variant *NPM1* mutations have been identified.[63] How the acquired NES changes the function of NPM in addition to altering the subcellular localization should be studied. The second question is why only *FLT3* mutations frequently accompany the *NPM1* mutation. According to a Japanese study, D835 of *FLT3* is also frequently mutated in *NPM1*-mutated AML. One possibility is that mutated NPM may sequester some transcription factors associated with differentiation. Activated *FLT3* might tyrosine-phosphorylate cytoplasmic NPM, which has been observed in NPM–ALK. Another possibility is that mutated NPM lowers the replication or repair fidelity of DNA. Umekawa *et al.* reported that the C-terminal sequence of NPM is important for its elevated DNA polymerase alpha activity compared with the short isoform NPM1.2.[71] As described below, *NPM1* haploinsufficiency increases the number of centrosomes to more than two and causes karyotype abnormalities in mice.[30] However, *NPM1* mutations are observed exclusively in AML with normal karyotype, and *FLT3* is the sole target for mutation. Recently Colombo *et al.* showed that mutant NPM forms a direct complex with Arf but is unable to protect it from degradation.[29] AML cells and cell lines harboring mutant NPM have low levels of cytoplasmic Arf. Colombo *et al.* suggested that inactivation of Arf, a key regulator of the

doi: 10.1111/j.1349-7006.2006.00270.x

Table 2. Clinical relevance of *NPM1* mutation in acute myeloid leukemia

Reference	Total patients (%) (normal karyotype)	Nucleophosmin mt (%) (normal ka ryotype)	Prognosis			
			CR	OS	EFS	RFS
Falini *et al.*[61]	591	35.2	F	NA	NA	NA
	(230)	(61.7)				
Suzuki *et al.*[65]	257	24.9	F	NS	NA	U
	(97)	(47.4)				
Boissel *et al.*[70]	(106)	(47)	NS	NS	NS	NS
Dohner *et al.*[68]	(300)	(48)	NS	NS	NA	F
Schittger *et al.*[66]	(401)	(52.9)	F	NS	F	NS
Verhaak *et al.*[67]	275	35	NA	NS	NS	NA
	(116)	(64)				
Thiede *et al.*[69]	1485	27.5	F	F	F	NA
	(709)	(45.7)			(DFS)	

CR, complete remission; DFS, disease-free survival; EFS, event-free survival; F, favorable; NS, not significant; OS, overall survival; RFS, relapse-free survival; U, unfavorable; NA, not analyzed.

p53-dependent cellular response to oncogene expression, might contribute to leukemogenesis in AML with mutated NPM. Further study is needed to clarify the underlying molecular mechanisms.

Haploinsufficiency and gene deletion in hematological malignancies

To study the function of NPM *in vivo*, Grisendi *et al.* generated *NPM1* heterozygous-null, hypomorphic-mutant and homozygous-null mice.[30] They observed that *NPM1* homozygous-null and hypomorphic mutants had aberrant organogenesis and died between embryonic days 11.5 and 16.5 owing to severe anemia resulting from defects in primitive hematopoiesis. They showed that *NPM1* inactivation leads to unrestricted centrosome duplication and genomic instability. Notably, *NPM1* heterozygous mice developed a hematological syndrome with features of human MDS. They concluded that their data uncovered an essential developmental role for NPM and implicated its functional loss in tumorigenesis and MDS pathogenesis.

According to the KO mice study, mutation or downregulation of *NPM1* as a tumor-suppressor gene may also be associated with human MDS. The evidence that *NPM1* is located on 5q35, which is deleted or rearranged in AML/MDS, suggests the loss of the *NPM1* gene in myeloid malignancies. Using fluorescence *in situ* hybridization and reverse transcription–polymerase chain reaction methods, Berger *et al.* analyzed eight AML/MDS cases with chromosomal breakpoints at 5q31–5q34.[72] Two bacterial artificial chromosome signals spanning the *NPM1* and *MLF1* genes were colocalized in three of the eight cases. However, the breakpoints were outside the *NPM1* gene in the remaining five cases, and one copy of the *NPM1* gene was deleted in three of the five. Further study is needed to determine the frequency and significance of *NPM1* deletion in the unbalanced translocation and chromosomal deletion.

Notably, the *NPM1* gene has a CpG island in its promoter region, which is potentially hypermethylated. However, no study has been reported about the methylation of the *NPM1* gene. The significance of promoter hypermethylation should also be investigated.

Conclusions and future directions

The *NPM1* gene is one of the most frequent targets for deletion and insertion mutations in addition to acting as a component of fusion genes. In fusion genes, translocation of the *NPM1* gene on the 5′ side is associated with ectopic expression, aberrant subcellular localization and oligomerization of the partner gene products. However, the biological significance of the *NPM1* gene mutation at exon 12 remains unclear. It may be associated with a mutator phenotype, dysregulated transcription or apoptosis. One interesting issue is altered nuclear–cytoplasmic trafficking of mutant NPM. The export system of mutant NPM might be a candidate for targeted therapy for NPM-mutated AML. Clarification of the expression and subcellular localization of NPM-interacting proteins such as p53, MDM2 and Arf in NPM-mutated AML would help to further our understanding of the pathogenesis of this disease. It would also yield insights into the masked function of NPM in myeloid hematopoiesis. The interaction between *FLT3* and *NPM1* mutations is another important issue for future studies. The evidence that *FLT3* and *NPM1* mutations are observed in a variety of types of AML from M0 to M7 (except M3) raises the question of what determines the phenotype of AML from M0 to M7. Thus, one discovery generates 10 more questions.

References

1 Lischwe M, Smetana K, Olson M *et al.* Protein-C23 and protein-B23 are the major nucleolar silver staining proteins. *Life Sci* 1979; **25**: 701–8.
2 Feuerstein N, Spiegel S, Mond JJ. The nuclear matrix protein, numatrin (B23), is associated with growth factor-induced mitogenesis in Swiss 3T3 fibroblasts and with T lymphocyte proliferation stimulated by lectins and anti-T cell antigen receptor antibody. *J Cell Biol* 1988; **107**: 1629–42.
3 Chan W-Y, Liu Q-R, Borjigin J *et al.* Characterization of the cDNA encoding human nucleophosmin and studies of its role in normal and abnormal growth. *Biochemistry* 1989; **28**: 1033–9.
4 Dalenc F, Drouet J, Ader I *et al.* Increased expression of a COOH-truncated nucleophosmin resulting from alternative splicing is associated with cellular resistance to ionizing radiation in HeLa cells. *Int J Cancer* 2002; **100**: 662–8.
5 International Human Genome Sequencing Consortium. Finishing the euchromatic sequence of the human genome. *Nature* 2004; **431**: 931–45.
6 Wang D, Umekawa H, Olson MO. Expression and subcellular locations of two forms of nucleolar protein B23 in rat tissues and cells. *Cell Mol Biol Res* 1993; **39**: 33–42.
7 Wang W, Budhu A, Forgues M, Wang XW. Temporal and spatial control of nucleophosmin by the Ran–Crm1 complex in centrosome duplication. *Nat Cell Biol* 2005; **7**: 823–30.
8 Morris SW, Xue L, Ma Z, Kinney MC. Alk+ CD30+ lymphomas: a distinct molecular genetic subtype of non-Hodgkin's lymphoma. *Br J Haematol* 2001; **113**: 275–95.
9 Pandolfi PP. *PML*, *PLZF* and *NPM* genes in the molecular pathogenesis of acute promyelocytic leukemia. *Haematologica* 1996; **81**: 472–82.
10 Yoneda-Kato N, Look AT, Kirstein MN *et al.* The t(3;5) (q25.1;q34) of myelodysplastic syndrome and acute myeloid leukemia produces a novel fusion gene, *NPM–MLF1*. *Oncogene* 1996; **12**: 265–75.
11 Okuda M. The role of nucleophosmin in centrosome duplication. *Oncogene* 2002; **21**: 6170–4.

12 Colombo E, Marine JC, Danovi D, Falini B, Pelicci PG. Nucleophosmin regulates the stability and transcriptional activity of p53. *Nat Cell Biol* 2002; 4: 529–33.
13 Szebeni A, Herrera JE, Olson MO. Interaction of nucleolar protein B23 with peptides related to nuclear localization signals. *Biochemistry* 1995; **34**: 8037–42.
14 Borer RA, Lehner CF, Eppenberger HM, Nigg EA. Major nucleolar proteins shuttle between nucleus and cytoplasm. *Cell* 1989; **56**: 379–90.
15 Dutta S, Akey IV, Dingwall C *et al.* The crystal structure of nucleoplasmin-core: implications for histone binding and nucleosome assembly. *Mol Cell* 2001; **8**: 841–53.
16 Huang N, Negi S, Szebeni A, Olson MO. Protein NPM3 interacts with the multifunctional nucleolar protein B23/nucleophosmin and inhibits ribosome biogenesis. *J Biol Chem* 2005; **280**: 5496–502.
17 Kondo T, Minamino N, Nagamura-Inoue T, Matsumoto M, Taniguchi T, Tanaka N. Identification and characterization of nucleophosmin/B23/numatrin which binds the anti-oncogenic transcription factor IRF-1 and manifests oncogenic activity. *Oncogene* 1997; **15**: 1275–81.
18 Hsu CY, Yung BY. Over-expression of nucleophosmin/B23 decreases the susceptibility of human leukemia HL-60 cells to retinoic acid-induced differentiation and apoptosis. *Int J Cancer* 2000; **88**: 392–400.
19 Kurki S, Peltonen K, Latonen L *et al.* Nucleolar protein NPM interacts with HDM2 and protects tumor suppressor protein p53 from HDM2-mediated degradation. *Cancer Cell* 2004; **5**: 465–75.
20 Sirri V, Roussel P, Gendron MC, Hernandez-Verdun D. Amount of the two major Ag-NOR proteins, nucleolin and protein B23, is cell-cycle dependent. *Cytometry* 1997; **28**: 147–56.
21 Okuda M, Horn HF, Tarapore P *et al.* Nucleophosmin/B23 is a target of CDK2/cyclin E in centrosome duplication. *Cell* 2000; **103**: 127–40.
22 Okuda M. The role of nucleophosmin in centrosome duplication. *Oncogene* 2002; **21**: 6170–4.
23 Cha H, Hancock C, Dangi S, Maiguel D, Carrier F, Shapiro P. Phosphorylation regulates nucleophosmin targeting to the centrosome during mitosis as detected by cross-reactive phosphorylation-specific MKK1/MKK2 antibodies. *Biochem J* 2004; **378**: 857–65.
24 Wu MH, Yung BY. UV stimulation of nucleophosmin/B23 expression is an immediate-early gene response induced by damaged DNA. *J Biol Chem* 2002; **277**: 48 234–40.
25 Zhang Y, Xiong Y. Control of p53 ubiquitination and nuclear export by MDM2 and ARF. *Cell Growth Diff* 2001; **12**: 175–86.
26 Brady SN, Yu Y, Maggi LB Jr, Weber JD. ARF impedes NPM/B23 shuttling in an Mdm2-sensitive tumor suppressor pathway. *Mol Cell Biol* 2004; **24**: 9327–38.
27 Bertwistle D, Sugimoto M, Sherr CJ. Physical and functional interactions of the Arf tumor suppressor protein with nucleophosmin/B23. *Mol Cell Biol* 2004; **24**: 985–96.
28 Korgaonkar C, Hagen J, Tompkins V *et al.* Nucleophosmin (B23) targets ARF to nucleoli and inhibits its function. *Mol Cell Biol* 2005; **25**: 1258–71.
29 Colombo E, Bonetti P, Lazzerini Denchi E *et al.* Nucleophosmin is required for DNA integrity and p19Arf protein stability. *Mol Cell Biol* 2005; **25**: 8874–86.
30 Grisendi S, Bernardi R, Rossi M *et al.* Role of nucleophosmin in embryonic development and tumorigenesis. *Nature* 2005; **437**: 147–53.
31 Sugimoto M, Kuo ML, Roussel MF, Sherr CJ. Nucleolar Arf tumor suppressor inhibits ribosomal RNA processing. *Mol Cell* 2003; **11**: 415–24.
32 Itahana K, Bhat KP, Jin A *et al.* Tumor suppressor ARF degrades B23, a nucleolar protein involved in ribosome biogenesis and cell proliferation. *Mol Cell* 2003; **12**: 1151–64.
33 Jaffe ES, Harris NL, Stein H, Vardiman JW, eds. *Pathology and Genetics of Tumors of Haematopoietic and Lymphoid Tissues*. Lyon, France: IARC Press, 2001.
34 Duyster J, Bai RY, Morris SW. Translocations involving anaplastic lymphoma kinase (ALK). *Oncogene* 2001; **20**: 5623–37.
35 Morris SW, Kirstein MN, Valentine MB *et al.* Fusion of a kinase gene, *ALK*, to a nucleolar protein gene, *NPM*, in non-Hodgkin's lymphoma. *Science* 1994; **263**: 1281–4.
36 Pulford K, Lamant L, Espinos E *et al.* The emerging normal and disease-related roles of anaplastic lymphoma kinase. *Cell Mol Life Sci* 2004; **61**: 2939–53.
37 Slupianek A, Nieborowska-Skorska M, Hoser G *et al.* Role of phosphatidylinositol 3-kinase-Akt pathway in nucleophosmin/anaplastic lymphoma kinase-mediated lymphomagenesis. *Cancer Res* 2001; **61**: 2194–9.
38 Ruchatz H, Coluccia AM, Stano P, Marchesi E, Gambacorti-Passerini C. Constitutive activation of Jak2 contributes to proliferation and resistance to apoptosis in NPM/ALK-transformed cells. *Exp Hematol* 2003; **31**: 309–15.
39 Turner SD, Alexander DR. What have we learnt from mouse models of NPM–ALK-induced lymphomagenesis? *Leukemia* 2005; **19**: 1128–34.
40 Stein H, Foss HD, Durkop H *et al.* CD30(+) anaplastic large cell lymphoma: a review of its histopathologic, genetic, and clinical features. *Blood* 2000; **96**: 3681–95.
41 Horie R, Watanabe T, Morishita Y *et al.* Ligand-independent signaling by overexpressed CD30 drives NF-κB activation in Hodgkin–Reed–Sternberg cells. *Oncogene* 2002; **21**: 2493–503.
42 Horie R, Watanabe M, Ishida T *et al.* The *NPM–ALK* oncoprotein abrogates CD30 signaling and constitutive NF-κB activation in anaplastic large cell lymphoma. *Cancer Cell* 2004; **5**: 353–64.
43 Cordell JL, Pulford KA, Bigerna B *et al.* Detection of normal and chimeric nucleophosmin in human cells. *Blood* 1999; **93**: 632–42.
44 Drexler HG, Gignac SM, von Wasielewski R, Werner M, Dirks WG. Pathobiology of *NPM–ALK* and variant fusion genes in anaplastic large cell lymphoma and other lymphomas. *Leukemia* 2000; **14**: 1533–59.
45 Piazza F, Gurrieri C, Pandolfi PP. The theory of APL. *Oncogene* 2001; **20**: 7216–22.
46 Zelent A, Guidez F, Melnick A, Waxman S, Licht JD. Translocations of the *RARα* gene in acute promyelocytic leukemia. *Oncogene* 2001; **20**: 7186–203.
47 Grimwade D, Biondi A, Mozziconacci MJ *et al.* Characterization of acute promyelocytic leukemia cases lacking the classic t(15;17): results of the European Working Party. *Blood* 2000; **96**: 1297–308.
48 Corey SJ, Locker J, Oliveri DR *et al.* A non-classical translocation involving 17q12 (retinoic acid receptor α) in acute promyelocytic leukemia (APML) with atypical features. *Leukemia* 1994; **8**: 1350–3.
49 Redner RL, Rush EA, Faas S, Rudert WA, Corey SJ. The t(5;17) variant of acute promyelocytic leukemia expresses a nucleophosmin–retinoic acid receptor fusion. *Blood* 1996; **87**: 882–6.
50 Redner RL, Corey SJ, Rush EA. Differentiation of t(5;17) variant acute promyelocytic leukemic blasts by all-trans retinoic acid. *Leukemia* 1997; **11**: 1014–16.
51 Redner RL, Chen JD, Rush EA, Li H, Pollock SL. The t(5;17) acute promyelocytic leukemia fusion protein NPM–RAR interacts with co-repressor and co-activator proteins and exhibits both positive and negative transcriptional properties. *Blood* 2000; **95**: 2683–90.
52 Sternsdorf T, Phan VT, Maunakea ML *et al.* Forced retinoic acid receptor α homodimers prime mice for APL-like leukemia. *Cancer Cell* 2006; **9**: 81–94.
53 Cheng GX, Zhu XH, Men XQ *et al.* Distinct leukemia phenotypes in transgenic mice and different corepressor interactions generated by promyelocytic leukemia variant fusion genes *PLZF–RARα* and *NPM–RARα*. *Proc Natl Acad Sci USA* 1999; **96**: 6318–23.
54 Dyck JA, Maul GG, Miller WH Jr, Chen JD, Kakizuka A, Evans RM. A novel macromolecular structure is a target of the promyelocyte–retinoic acid receptor oncoprotein. *Cell* 1994; **76**: 333–43.
55 Raelson JV, Nervi C, Rosenauer A *et al.* The PML/RARα oncoprotein is a direct molecular target of retinoic acid in acute promyelocytic leukemia cells. *Blood* 1996; **88**: 2826–32.
56 Yoshida H, Kitamura K, Tanaka K *et al.* Accelerated degradation of PML–retinoic acid receptor alpha (PML–RARA) oncoprotein by all-trans-retinoic acid in acute promyelocytic leukemia: possible role of the proteasome pathway. *Cancer Res* 1996; **56**: 2945–8.
57 Rush EA, Schlesinger KW, Watkins SC, Redner RL. The NPM–RAR fusion protein associated with the t(5;17) variant of APL does not interact with PML. *Leuk Res* 2006; **30**: 979–86.
58 Winteringham LN, Kobelke S, Williams JH, Ingley E, Klinken SP. Myeloid leukemia factor 1 inhibits erythropoietin-induced differentiation, cell cycle exit and p27Kip1 accumulation. *Oncogene* 2004; **23**: 5105–9.
59 Hanissian SH, Akbar U, Teng B *et al.* cDNA cloning and characterization of a novel gene encoding the MLF1-interacting protein MLF1IP. *Oncogene* 2004; **23**: 3700–7.
60 Falini B, Bigerna B, Pucciarini A *et al.* Aberrant subcellular expression of nucleophosmin and NPM–MLF1 fusion protein in acute myeloid leukaemia carrying t(3;5): a comparison with NPMc+ AML. *Leukemia* 2006; **20**: 368–71.
61 Falini B, Mecucci C, Tiacci E *et al.* Gimema Acute Leukemia Working Party. Cytoplasmic nucleophosmin in acute myelogenous leukemia with a normal karyotype. *N Engl J Med* 2005; **352**: 254–66.
62 Nakagawa M, Kameoka Y, Suzuki R. Nucleophosmin in acute myelogenous leukemia. *N Engl J Med* 2005; **352**: 1819–20.
63 Falini B, Bolli N, Shan J *et al.* Both carboxy-terminus NES motif and mutated tryptophan(s) are crucial for aberrant nuclear export of nucleophosmin leukemic mutants in NPMc+ AML. *Blood* 2006; **107**: 4514–23.
64 Grisendi S, Pandolfi PP. NPM mutations in acute myelogenous leukemia. *N Engl J Med* 2005; **352**: 291–2.
65 Suzuki T, Kiyoi H, Ozeki K *et al.* Clinical characteristics and prognostic implications of NPM1 mutations in acute myeloid leukemia. *Blood* 2005; **106**: 2854–61.
66 Schnittger S, Schoch C, Kern W *et al.* Nucleophosmin gene mutations are predictors of favorable prognosis in acute myelogenous leukemia with a normal karyotype. *Blood* 2005; **106**: 3733–9.
67 Roel GWV, Chantal SG, Wim van P *et al.* Mutations in nucleophosmin (NPM1) in acute myeloid leukemia (AML): association with other gene

doi: 10.1111/j.1349-7006.2006.00270.x

abnormalities and previously established gene expression signatures and their favorable prognostic significance. *Blood* 2005; **106**: 3747–54.
68 Konstanze D, Richard FS, Marianne H *et al.* Mutant nucleophosmin (NPM1) predicts favorable prognosis in younger adults with acute myeloid leukemia and normal cytogenetics: interaction with other gene mutations. *Blood* 2005; **106**: 3740–6.
69 Christian T, Sina K, Eva C *et al.* Prevalence and prognostic impact of NPM1 mutations in 1485 adult patients with acute myeloid leukemia (AML) *Blood* 2006; **107**: 4011–20.
70 Boissel N, Renneville A, Biggio V *et al.* Prevalence, clinical profile, and prognosis of NPM mutations in AML with normal karyotype. *Blood* 2005; **106**: 3618–20.
71 Umekawa H, Sato K, Takemura M *et al.* The carboxyl terminal sequence of nucleolar protein B23.1 is important in its DNA polymerase α-stimulatory activity. *J Biochem (Tokyo)* 2001; **130**: 199–205.
72 Berger R, Busson M, Baranger L *et al.* Loss of the *NPM1* gene in myeloid disorders with chromosome 5 rearrangements. *Leukemia* 2006; **20**: 319–21.
73 Namboodiri VM, Akey IV, Schmidt-Zachmann MS, Head JF, Akey CW. The structure and function of *Xenopus* NO38-core, a histone chaperone in the nucleolus. *Structure* 2004; **12**: 2149–60.

ELSEVIER

Cancer Genetics and Cytogenetics 169 (2006) 1–11

CANCER GENETICS AND CYTOGENETICS

Establishment of a myeloid leukemia cell line, TRL-01, with *MLL-ENL* fusion gene

Manabu Ninomiya[a,1], Akihiro Abe[a,1], Toshiya Yokozawa[b], Kazutaka Ozeki[a], Kazuhito Yamamoto[c], Mamoru Ito[d], Masafumi Ito[e], Hitoshi Kiyoi[f], Nobuhiko Emi[a], Tomoki Naoe[a,*]

[a]*Department of Hematology, Nagoya University Graduate School of Medicine, 65 Tsurumai-cho, Showa-ku, Nagoya 466-8550, Japan*
[b]*Division of Hematology, Nagoya Medical Center, National Hospital Organization, 4-1-1 Sannomaru, Naka-Ku, Nagoya, Japan*
[c]*Department of Preventive Medicine/Biostatics and Medical Decision Making, Nagoya University Graduate School of Medicine, Nagoya, Japan*
[d]*Central Institute for Experimental Animals, 1430 Nogawa, Miyamae-ku, Kawasaki, Japan*
[e]*Department of Pathology, Japanese Red Cross Nagoya First Hospital, 3-35 Michisita-cho, Nakamura-ku, Nagoya, Japan*
[f]*Department of Infectious Diseases, Nagoya University Hospital, 65 Tsuramai-cho, Showa-ku, Nagoya, Japan*

Received 21 July 2005; received in revised form 8 September 2005; accepted 9 September 2005

Abstract We established a leukemia cell line derived from therapy-related acute myeloid leukemia with the t(11;19) by xenotransplantation into the NOD/SCID mouse with IL-2Rγ_c−/− (NOG mouse). The cell line, TRL-01, could be serially transplanted from mouse to mouse and also grown in an adherence-dependent manner on a murine bone marrow stroma cell line, HESS-5. TRL-01 had the same immunophenotype as the original leukemia cells: positive for CD13, CD33, CD11a, CD18, CD29, CD49d, CD49e, CD54, CD62L, and CD117, and negative for CD3, CD4, CD8, CD19, CD34, CD41a, CD41b, CD135, and myeloperoxidase. Translocation (11;19)(q23;p13) in both the original sample and TRL-01 generated *MLL-ENL* chimeric transcripts joining exon 6 and exon 4, respectively, which has a novel isoform. In cultures of TRL-01, addition of GM-CSF, SCF, and G-CSF and adhesion to fibronectin-coated plates promoted transient proliferation and survival, although they did not support long-term culture. Subcutaneous injection caused a tumor to form only when HESS-5 was coinjected at the same site. These results suggest that TRL-01 is a useful cell line for studying not only the leukemia-related biology of *MLL-ENL* but also the intercellular association between leukemia and stroma.

1. Introduction

Leukemia cell lines are indispensable tools in the study of research of leukemia. Many cell lines have contributed to advances in basic biology or to therapeutic development [1]. Nevertheless, the cell lines are different from leukemia cells in vivo. For example, leukemia cells removed from their environment (e.g., bone marrow [BM]) usually undergo apoptosis within a few weeks even if cultured carefully. Moreover, during the process of establishing cell lines, a variety of events may intrude, singly or in combination: a small population of leukemia cells may be selected, transcriptional control may change, or genomic alterations may be accumulated [2,3]. A new culture system is needed, one that is more similar to the native environment.

Recently, immunodeficient mice have been generated to study leukemia in terms of cellular origin, pathogenesis, and approaches to therapy. Such models have the advantage of allowing the cellular biology of leukemia to be investigated, especially the leukemia–microenvironment interaction [4–6]. So far, however, it has been impossible to maintain human leukemia cells long term by passage from mouse to mouse, although there are many reports on xenotransplantation of human leukemia into mice. To generate more immunodeficient mice, the common γ chain gene or β_2-microglobulin gene has been knocked out in NOD/SCID mice [7]. In cord blood xenotransplantation, engraftment with excellent efficacy and differentiation into all lineages, including T cells, were observed [8]; however, the efficacy of engraftment using clinical samples has not fully been

[1] These authors are equal contributors.

* Corresponding author. Tel. and fax: +81-52-744-2136.
E-mail address: tnaoe@med.nagoya-u.ac.jp (T. Naoe).

0165-4608/06/$ – see front matter © 2006 Elsevier Inc. All rights reserved.
doi:10.1016/j.cancergencyto.2005.09.008

investigated. We have transplanted fresh leukemia cells into NOG mice to establish an animal model of leukemia.

Here we established a leukemia cell line derived from therapy-related acute myeloid leukemia with the t(11;19) by xenotransplantation into NOG mice. The cell line could be serially transplanted from mouse to mouse and also grown in an adherence-dependent manner on a murine bone marrow stroma cell line, HESS-5.

2. Materials and methods

2.1. Patient

A 34-year-old Japanese woman was admitted to our hospital because of pancytopenia and detection of peripheral blasts in March 2003. From March 1997 through April 2001, she was treated with a succession of chemotherapies including etoposide (a total dose of 32.9 g), actinomycin-D, methotrexate, cisplatin, carboplatin, cyclophosphamide, ifosfamide, and vincristine against recurrent choriocarcinoma. Her BM blasts were peroxidase-negative and CD13+, CD33+, CD3−, CD4−, CD5−, CD56−, CD7+, CD19−, CD34−, CD14−, CD11b−, CD10−, CD41b−, CD41a−. The karyotype was 46,XX,t(11;19)(q23;p13),add(12)(p11)[10]/46, idem,i(21)(q10)[5]/46,idem,add(21)(q22)[5] in 20 metaphases examined. She was diagnosed with topoisomerase II inhibitor-related acute myeloid leukemia (AML) according to the WHO classification. Hematological remission was achieved by chemotherapy with idarubicin and cytarabine, but the truncal skin was involved 2 months later. She received an allogeneic peripheral stem cell transplantation in July 2003, but died of graft failure and pneumonia in September 2003.

2.2. Cells

The BM cells from the patient were collected after obtaining informed consent. Mononuclear cells (MNC) were separated by Ficoll-Paque Plus (Amersham Bioscience, Uppsala, Sweden) density-gradient centrifugation, and used as BM MNCs for the transplantation procedure. Some of the cells were cultivated in RPMI 1640 medium (Gibco-BRL, Gaithersburg, MD) supplied with 20 % fetal bovine serum (Gibco-BRL), 100 IU/mL of penicillin G (Meiji Seika, Tokyo, Japan), and 100 μg/mL of streptomycin (Meiji Seika). The murine BM stroma cell line MS-5 was maintained in α-minimum essential medium (α-MEM; Gibco-BRL) supplemented with 20% horse serum (Gibco-BRL), 100 IU/mL of penicillin G, and 100 μg/mL of streptomycin. The murine BM stroma cell line HESS-5 was maintained in Dulbecco's minimal essential medium (DMEM; Gibco-BRL) supplemented with 10% horse serum, 100 IU/mL of penicillin G, and 100 μg/mL of streptomycin. The monkey kidney-derived epithelial-like cell line COS-7, human kidney-derived epithelial-like cell line 293T, and murine embryo-derived fibroblast-like cell line NIH3T3 were maintained in DMEM supplemented with 10% fetal bovine serum, 100 IU/mL of penicillin G, and 100 μg/mL of streptomycin. The newborn murine calvaria-derived fibroblast-like cell line OP9 was maintained in α-MEM supplemented with 20% fetal bovine serum, 100 IU/mL of penicillin G, and 100 μg/mL of streptomycin. Human precursor B-cell ALL cell line RS4;11 with t(4;11) was obtained from the American Type Culture Collection (ATCC, Rockville, MD). The cell lines were cultivated in RPMI-1640 medium supplemented with 10% fetal bovine serum, 100 IU/mL of penicillin G, and 100 μg/mL of streptomycin.

2.3. Mice and transplantation procedure

NOG mice, generated by backcrossing NOD/SCID mice with C57BL6J-γ_c−/− mice as described [7], were maintained at the Central Institute for Experimental Animals (Kawasaki, Japan). The BM MNCs (2×10^6 cells) were injected into nonirradiated 7- to 8-week-old male mice via a tail vein. In the serial passage experiment, the spleen was extirpated from the engrafted mice after ether anesthesia. Cell suspension was prepared from the spleen, then it was adjusted to 2×10^6 cells and injected into nonirradiated 7- to 8-week-old male mice via a tail vein. We repeated the procedure at 8-week intervals. The animal experiments were approved by the institutional ethics committee for Laboratory Animal Research, Nagoya University School of Medicine and were performed according to the guidelines of the Institute.

2.4. Phenotypic analyses

Flow-cytometric analyses were performed according to a method described below. NOG mice at 8 weeks after transplantation were killed under ether anesthesia, and then the major organs were removed. Cell suspensions from BM and spleen were prepared and subjected to flow cytometry. To detect human cells from the tissues, a multicolor cytometric analysis was performed using FACScalibur (Becton Dickinson [BD], Franklin Lakes, NJ), according to the manufacturer's direction. Samples were mixed and incubated with an appropriate volume of antibodies for 30 minutes on ice. These cells were examined by staining with a combination of 7-AAD (BD PharMingen) for the live gate, and either or both of phycoerythrin (PE)-conjugated antibody and fluorescein isothiocyanate (FITC)-conjugated antibody. The PE-conjugated antibodies used were anti-human CD3, CD19, CD33, CD34 antibodies (BD, San Jose, CA), anti-human CD56 antibody (BD Pharmingen). The FITC-conjugated antibody was anti-human CD45 antibody (BD). FITC and PE-labeled isotype control antibodies (BD) were also used.

For the evaluation of the surface marker of TRL-01, the cells were stained with a combination of PerCP-conjugated anti-human CD45 antibody (BD) for the CD45 gate and either or both of PE-conjugated antibodies and FITC-conjugated antibody. The PE-conjugated antibodies used were anti-human CD11b, CD13, CD14, CD18, CD29,

CD44, CD49d, CD49e antibodies (BD), and anti-human CD117, CD135 antibodies (Beckman Coulter, San Jose, CA). The FITC-conjugated antibody used was anti-human CD41 antibody (BD). An additional reaction with FITC and PE-labeled isotype control antibodies (BD) was performed as a negative control. Analyses were performed using Cell Quest software (BD).

2.5. Karyotype and dual-color fluorescence in situ hybridization analyses

Karyotyping was performed as described previously [9]. Briefly, the BM or spleen cells from NOG mice were cultured for 24 hours. Twenty G-banded metaphases were analyzed according to standard procedures. Dual-color fluorescence in situ hybridization (DC-FISH) analyses were performed as described previously [9], using an LSI MLL dual-color break-apart rearrangement probe consisting of a 350-kbp portion of the *MLL* gene breakpoint cluster region (bcr) labeled in SpectrumGreen and an ~190-kbp portion largely telomeric of the bcr labeled in SpectrumOrange (Vysis, Abbott Laboratories, Abbott Park, IL). The translocation signals were evaluated using a fluorescence microscope with triple-pass filters (Nikon, Tokyo, Japan). At least 500 cells without damaged nuclei were blindly counted in each sample. Less than 1% of the total cell population failed to show hybridization. Only those spots with a similar size, intensity, and shape were counted. A fusion spot was scored as a normal *MLL* allele (negative for the MLL translocation); split signals of green and orange were scored as positive for the *MLL* translocation.

2.6. Reverse transcription-polymerase chain reaction (RT-PCR)

For reverse transcription polymerase chain reaction (RT-PCR), total RNA was prepared from the spleen of mouse and BM MNCs using a QIAamp RNA blood mini kit (Qiagen, Chatsworth, CA) as previously described [10]. Briefly, cDNA was synthesized from extracted RNA using random primer, dNTP, Superscript II (reverse transcriptase; Gibco-BRL), dithiothreitol, and $MgCl_2$ in a final volume of 20 μL at 42°C for 40 min. The 1 μL cDNA was amplified with 0.2 mmol/L dNTP, 1.25 U AmpliTaq Gold (DNA polymerase; Perkin-Elmer, Norwalk, CT), and 0.5 μmol/L primers in 50-μL reaction volumes using a GeneAmp PCR System 9600 (Perkin Elmer). Each thermal cycle to detect *MLL-ENL* [11], *MLL-ELL* [12], or *MLL-MEN* [13] was performed according to the described method with 35 cycles. Primers were synthesized by Nihon Gene Research Lab (Sendai, Japan); for the sequences of the primers in *MLL-ENL*, see the Supplemental Data section. PCR products were separated on 1.5% agarose gels and visualized by ethidium bromide staining and photographed on a UV transilluminator FASIII (Toyobo, Tokyo, Japan).

2.7. cDNA panhandle PCR

Panhandle PCR was performed with the described method [14,15]. Total RNA was prepared from TRL-01 using a QIAamp RNA blood mini kit (Qiagen). First-strand cDNAs were synthesized from 1 μg of total RNA by using the Superscript preamplification system (Life Technologies, Grand Island, NY), using *MLL*-random hexamer oligonucleotides (5′-CCTGAATCCAAA-CAGGCCACCACTCCAGCTTC-NNNNNN-3′); the *MLL* sequence in the oligonucleotides corresponded to breakpoint cluster region (bcr) cDNA positions 92–123 in exon 5. Two microliters of first-strand cDNAs was added to a 45.5-μL mixture containing 1.75 units of AmpliTaq Gold (DNA polymerase; Perkin Elmer), 385 μmol/L of each dNTP, 1.1× buffer, and 12.5 pmol of *MLL* primer 1. The mixture was heated to 80°C for 5 min before the cDNAs were added.

Primer 1 corresponded to *MLL* bcr cDNA positions 34–55 in exon 5 (5′-TCCTCCACGAAAGCCCGTC-GAG-3′), upstream of the *MLL* sequence in the oligonucleotides used to synthesize the first-strand cDNAs. To achieve primer 1 extension, the mixture was denatured at 94°C for 1 min. This was followed by 1 cycle at 94°C for 10 sec and 68°C for 7 min. The sample was heated again to 80°C for 5 min and 2.5 μL (12.5 pmol) of *MLL* primer 2 was added.

Primer 2 corresponded to *MLL* bcr cDNA positions 136–158 in exon 5 (5′-TCAAGCAGGTCTCCCAGCCAG-CAC-3′), downstream of the *MLL* sequence in the oligonucleotides used to synthesize the first-strand cDNAs. The final 50-μL PCR mixtures contained 350 μmol/L of each dNTP and 1× buffer.

PCR with primers 1 and 2, including the 7-min elongation and the incremental increase in the elongation period, was performed as described. One microliter of the products was used in nested PCR with primers 3 (5′-GGAAAA-GAGTGAAGAAGGGAATGTCTCGG-3′) and 4 (5′-GTGGTCATCCCGCCTCAGCCAC-3′) corresponding to *MLL* bcr cDNA positions 55–83 and 159–179 in exon 5. Conditions were the same as described above.

Panhandle PCR products were cloned into the plasmid vector, pBluescript SK(−) (Stratagene, La Jolla, CA), and the transformation was performed with DH5α cells (Life Technologies) according to the manufacturer's instructions. Subclones containing cDNA panhandle PCR products were identified by PCR with *MLL* primer 2 and primer 4. The resulting PCR fragments were sequenced by using the BigDye terminator cycle sequencing kit (Applied Biosystems, Foster City, CA) and analyzed with an ABI PRISM 310 genetic analyzer (Applied Biosystems).

For the detection of *MLL-ENL* transcripts of TRL-01, RT-PCR was performed. Total RNA was converted to single-stranded cDNA using oligo(dT) primers and MMLV-RT (Perkin Elmer). The resulting first-strand cDNA was amplified with *MLL* primer 4 and *ENL* primer 1 (5′-GGATGGTTTGGTCTTCTTGGGGTCAG-3′) by the use

of a Perkin Elmer GeneAmp 2400 thermocycler (Applied Biosystems).

2.8. Pathological examination

To evaluate morphological status, the extracted tissues were fixed with 10% formalin, and 4-μm sections mounted on slides were stained with hematoxylin and eosin (H&E). For immunohistochemical staining of human CD45, a LSAB2 system (DAKO Cytomation, Kyoto, Japan) using anti-human CD45 mouse monoclonal antibody (DAKO Cytomation) was used according to the instructions of an automatic immunohistochemical stainer (DAKO Cytomation).

2.9. Stroma-dependent growth in vivo

NOG mice were subcutaneously injected with 2×10^6 cells of TRL-01 and 6×10^4 cells of HESS-5 into dorsal regions. As controls, either 2×10^6 cells of TRL-01 alone or 6×10^4 cells of HESS-5 alone were similarly injected. The major axis (D, in mm) and minor axis (d, in mm) of the subcutaneous tumor was measured with vernier calipers, and the weight (mg) of the tumor was calculated with the formula $D \times d^2/2$ [16]. Human CD45 immunostaining and RT-PCR with *MLL-ENL* primers was performed to confirm the subcutaneous tumor to be involving of TRL-01 cells.

2.10. Proliferation and survival of the cells

The proliferation of the cells was profiled with a hemocytometer. The survival of the cells was examined using the trypan blue dye exclusion method. The requirement of direct adherence was estimated as follows. TRL-01 cells, adjusted to 1×10^5/mL, were seeded into a 6-well culture plate (BD), which was precultured with 5×10^3/mL of HESS-5 cells. The cell number and survival was estimated at 0, 3, and 7 days. After a BD cell culture insert (6-well format), which is a 0.4-μm porous membrane, had settled in the HESS-5 monolayer of the 6-well plate, 5×10^5 TRL-01 cells were seeded onto the insert. Total volume was adjusted to 5 mL in each well. The proliferation and survival was estimated during 7 days and was compared with the culture without a cell culture insert as a control. To investigate the

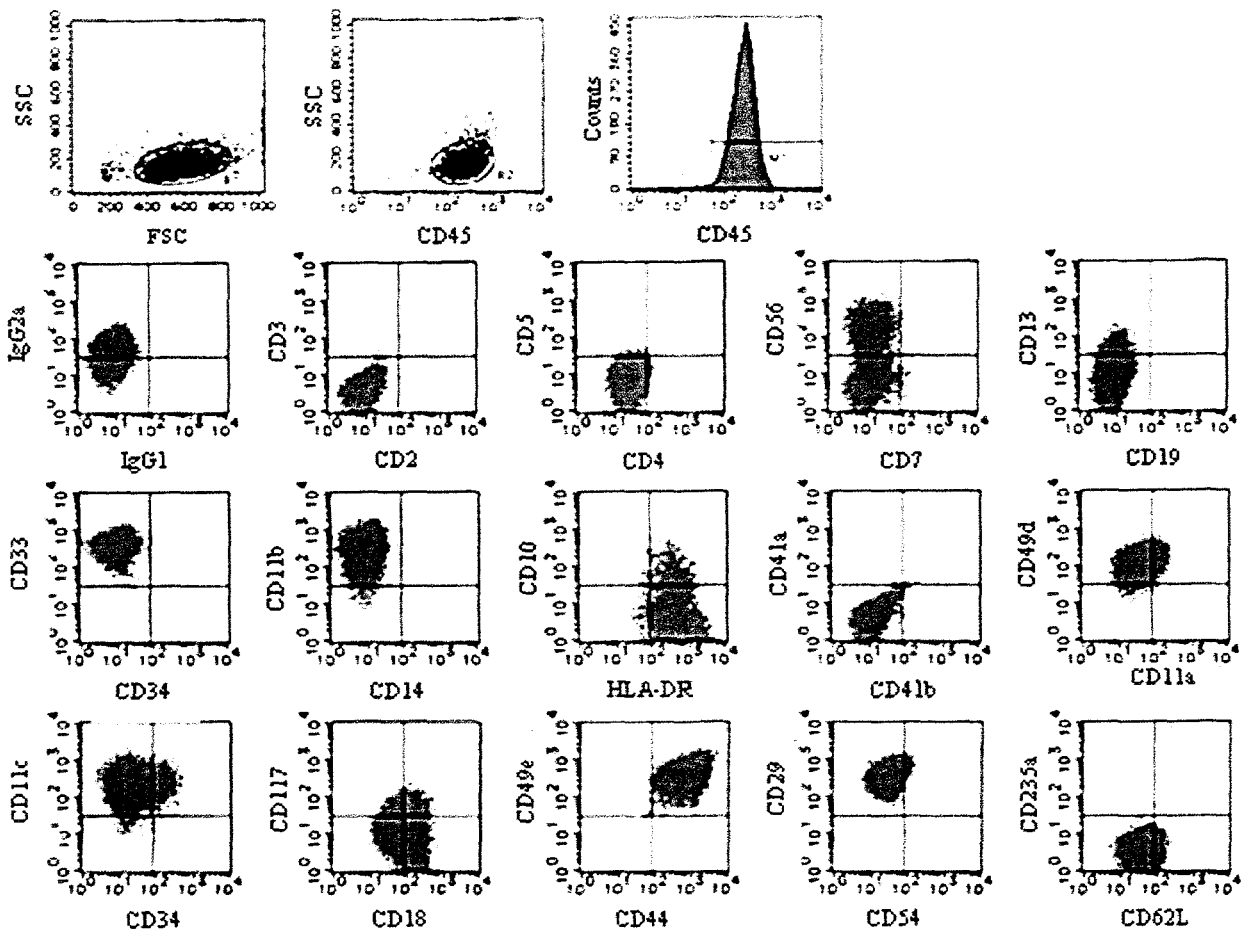

Fig. 1. Flow-cytometric analyses of the cells from the spleen of an engrafted NOG mouse 8 weeks after transplantation of BM MNCs from the AML M0 patient.

effect of the growth factors, TRL-01 cells were adjusted to 1×10^5/mL, and seeded into BioCoat (human fibronectin coated 6-well plate; BD). Then, 50 ng/mL of stem cell factor (SCF; Kirin, Tokyo, Japan), granulocyte macrophage-colony stimulating factor (GM-CSF; Kirin), granulocyte-colony stimulating factor (G-SCF; Kirin), thrombopoietin (TPO; Kirin), or erythropoietin (EPO; Kirin) was added to the culture. Differentiation was evaluated by flow-cytometric analysis using the labeled antibodies, and morphological changes of TRL-01 cells were detected by examining cytospin specimens subjected to May–Gruenwald's Giemsa staining and peroxidase–Giemsa staining.

2.11. Apoptosis detection

Apoptosis of TRL-01 cells was examined with FACScalibur using an Annexin V-FITC apoptosis detection kit (BD Pharmingen) according to the manufacturer's directions. Briefly, TRL-01 cells, adjusted to 1×10^5/mL, were seeded into a 6-well culture plate (BD), which was precultured with 5×10^3/mL of HESS-5 cells, BioCoat, or nontreated plate. The percentage of apoptosis was estimated using FACScalibur (BD) at 7 days. Analyses were performed using Cell Quest software (BD).

2.12. Statistics

Each experiment of proliferation, survival, and detection of apoptosis was repeated three times. Significant differences were calculated using the Student's *t*-test.

3. Results

The BM MNCs prepared from the leukemia patient were transplanted into NOG mice. Eight weeks later, the BM cells were replaced with human CD45-positive cells, which were passed at 8-week intervals for more than one year. The cells collected from the BM or spleen did not proliferate alone in medium but could be cultured on a BM stroma cell line, HESS-5. The doubling time was in the range of 3–4 days. TRL-01 in culture was able to be passed every week. This cell line was designated as TRL-01 and used for the subsequent experiments.

TRL-01 showed a basophilic cytoplasm, had round or indented nuclei with a fine nucleoreticulum, and was found to be negative for peroxidase and weakly positive for α-naphthyl acetate esterase. TRL-01 was found to be positive for myeloid markers of CD13 and CD33 and negative for lymphoid, monocytoid, erythroid, and megakaryocytoid markers, which was the same as the original leukemia cells ($CD13^+$, $CD33^+$, $CD3^-$, $CD4^-$, $CD5^-$, $CD56^-$, $CD7^+$, $CD19^-$, $CD34^-$, $CD14^-$, $CD11b^-$, $CD10^-$, $CD41b^-$, $CD41a^-$). Other markers were $CD11a^{low/-}$, $CD11b^+$, $CD18^{+/low}$, $CD29^+$, $CD44^+$, $CD49e^+$, $CD49d^+$, $CD54^{low}$, $CD56^{+/-}$, $CD62L^{low}$, $CD117^+$, HLA-DR$^+$ (Fig. 1), which was also the same as the BM MNCs used for the injection of NOG mice (data not shown).

Following serial passage in NOG mice, TRL-01 cells were detected in the BM within 1 month after injection, and in the spleen and mesenterium 1 month later but rarely found in other organs ($n = 5$; data not shown). The injected mice survived >4 months without cachexia.

Analysis of 20 metaphases revealed the presence of two clones in TRL-01 cells: 46,XX,t(11;19)(q23;p13.3), add(12)(p11.2)[4]/45,idem,der(2)t(2;15)(q35;q15),−15[16] (Fig. 2A). The occurrence of clonal evolution during the in vivo passage was suggested with the result of G-band analysis. The 46,idem,i(21)(q10) and 46,idem,add(21)(q22) detected at diagnosis were lost and a 45,idem,der(2) t(2;15)(q35;q15),−15 was generated in TRL-01. The *MLL*

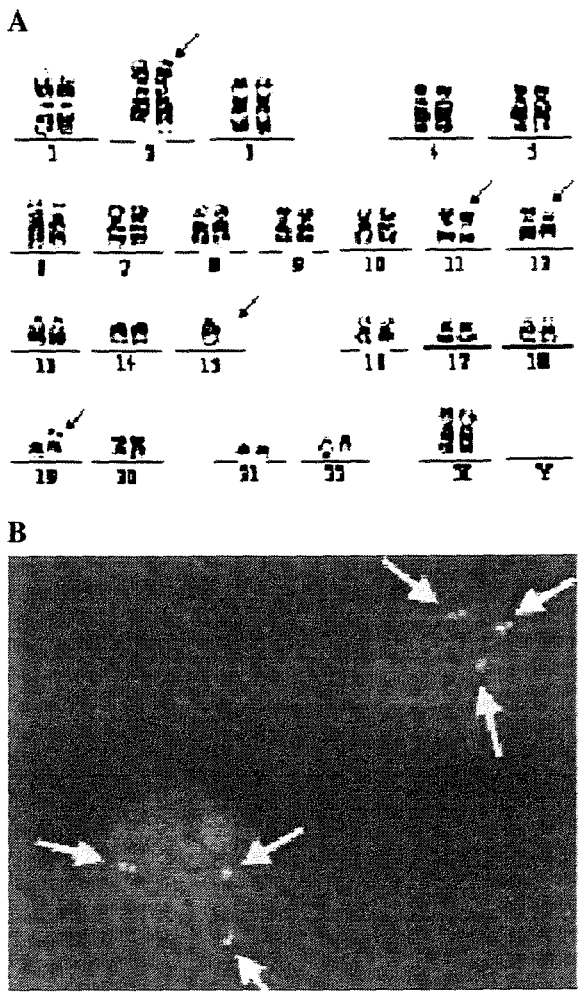

Fig. 2. Karyotypic and dual-color fluorescence in situ hybridization (DC-FISH) analyses. (A) Karyotype of TRL-01. Arrows indicate chromosomal alterations. (B) DC-FISH analyses were performed as described in the Materials and Methods section. Locus-specific probes for *MLL* gene breakpoint cluster region (bcr) labeled in SpectrumGreen and an ~190-kbp portion largely telomeric of the bcr labeled in SpectrumOrange were used. Cells with a fusion spot indicate a normal *MLL* allele (white arrows); split signals of green and orange are indicative of the *MLL* translocation (yellow arrows).

gene translocation was identified by DC-FISH analyses using a locus-specific probe for the *MLL* gene bcr labeled in SpectrumGreen and the telomeric bcr labeled in SpectrumOrange in the original AML cells and TRL-01 cells (Fig. 2B). This data suggested that the *MLL* gene, which is located at 11q23, was fused to a partner gene located at 19p13.

Because three kinds of fusion genes (*MLL-ENL*, *MLL-ELL*, and *MLL-MEN*) have been known in t(11;19)(q23;p13) [12,13,17], we amplified these fusion cDNAs by RT-PCR using appropriate primers; however, no bands were amplified (data not shown). We then applied the cDNA panhandle PCR method to obtain the fusion transcripts of *MLL*. Several PCR products were amplified in TRL-01 cells and the BM MNCs at diagnosis. The sequence of the PCR products revealed that exon 6 of the *MLL* gene (11q23) fused to exon 4 of the *ENL* gene (19p13.3), a breakpoint that has not been reported previously (Fig. 3A). The other cDNA panhandle PCR products had the wild-type *MLL* (data not shown). With the *MLL* primer 4 and *ENL* primer 1 (see Supplemental Data), a 438-bp PCR product was confirmed during the four

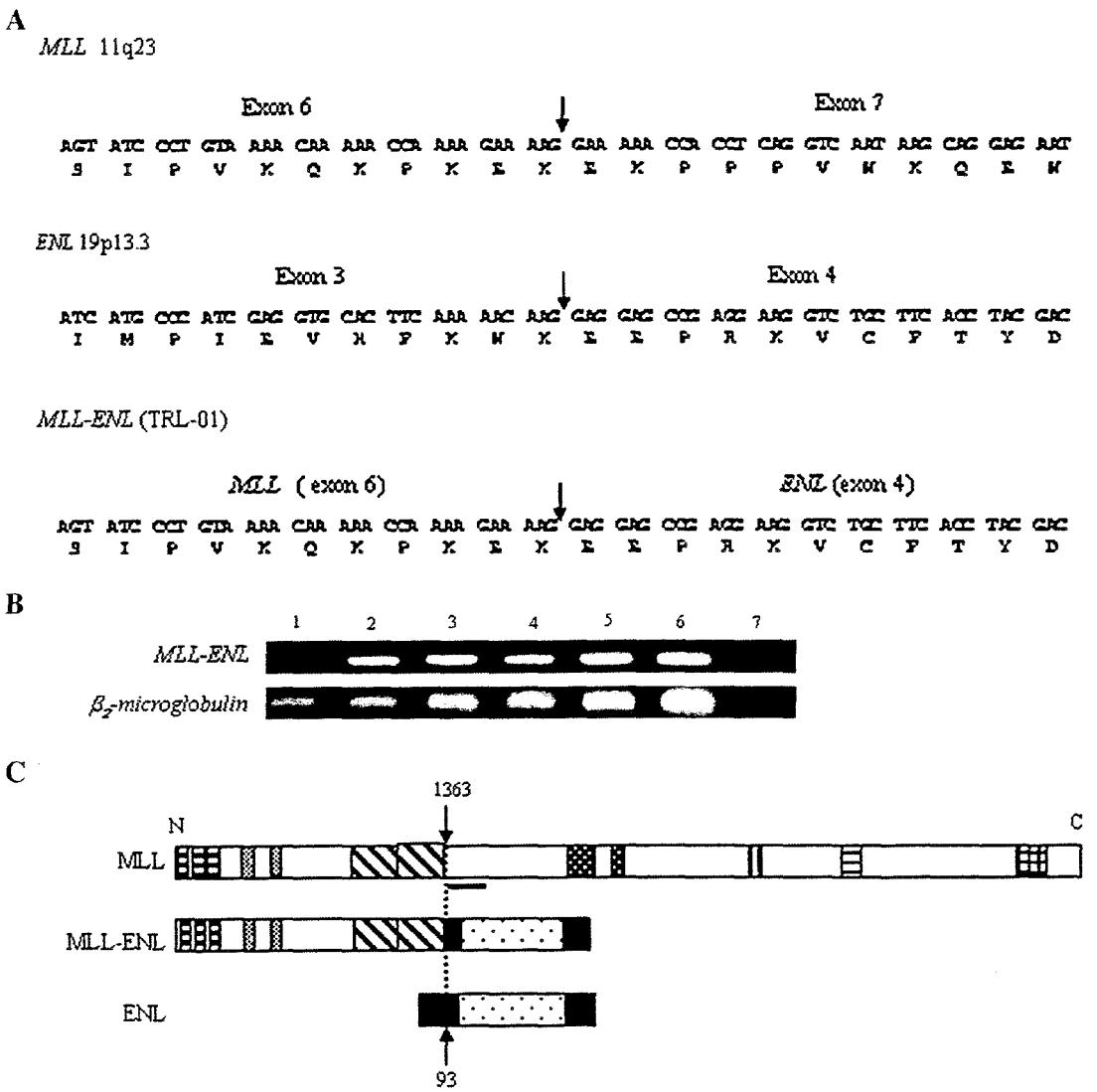

Fig. 3. Sequence of the cloned panhandle PCR product from TRL-01. (A) Normal sequence of *MLL* exon 6–exon 7, *ENL* exon 3–exon 4, and sequence of TRL-01. Arrows indicate the exon–exon boundaries. (B) RT-PCR of the *MLL-ENL* cDNA. Primers were *MLL* primer 4 and *ENL* primer 1, which gave PCR products at 438 bp. Lane 1, RS4;11; lane 2, BM MNC at diagnosis; lane 3, the spleen cells from NOG mouse in 1st passage; lane 4, the spleen cells from NOG mouse in 2nd passage; lane 5, the spleen cells from NOG mouse in 3rd passage; lane 6, the spleen cells from NOG mouse in 4th passage; lane 7, H_2O. As a positive control, primers for β_2-microglobulin were used. (C) Schematic representation of MLL, MLL-ENL, and ENL proteins: *Banding legend (left to right):* dark horizontal lines, AT hook; dotted white on gray, SNL1 and SNL2; slanted lines, repression domains (RD1 and RD2); closely dotted white on black, PHD zinc finger; vertical line, cleavage site; light horizontal lines, transactivation domain; and checkered, SET domain. The dark horizontal line below indicates the breakpoint cluster region of MLL. Solid black, ANC-1 homologous region; white, serine-proline rich region of ENL.

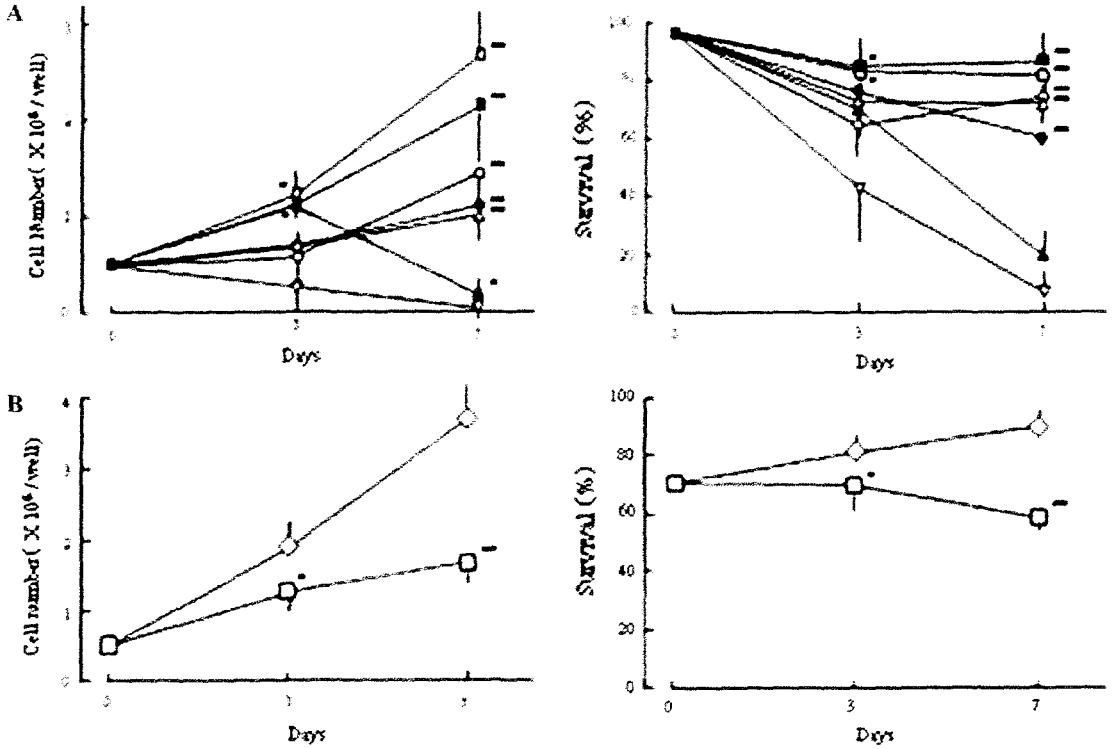

Fig. 4. TRL-01 required direct adhesion to specific stroma cells for growth. TRL-01 cells (1×10^5/mL, 5 mL) cultivated on MS-5 (open squares), HESS-5 (solid squares), OP-9 (open triangles up), COS-7 (solid circles), 293T (open circles), or NIH3T3 (solid triangles up) cells (5×10^3/mL), and no stroma cells (open triangles down) in 6-well plates for 7 days. (A) Data indicate cell number (left panel) and survival (%) (right panel). (B) Cultivation of TRL-01 (1×10^5/mL, 5 mL) on HESS-5 monolayer (5×10^3/mL) in 6-well plates with (open squares) or without (open diamonds) use of cell culture inserts for 7 days. Data indicate cell number (left panel) and survival (%) (right panel). **, $P<0.01$; *, $P<0.05$.

passages in the NOG mice (Fig. 3B). This result indicated that TRL-01 cells bearing t(11;19) stably maintained in the NOG mice environment.

We cultivated TRL-01 on various BM stroma cell lines to study which supported survival and growth of TRL-01 ex vivo. The best conditions were obtained in the culture with HESS-5 and MS-5 both of which are derived from mouse BM stroma cells ($n = 3$, $P < 0.01$; Fig. 4A). TRL-01 cells proliferated with a doubling time of 3–4 days, and the rate of cell survival remained >80%. COS-7, OP-9, and 293T cells partially stimulated the proliferation, with a doubling time of 5–7 days, whereas survival was moderately maintained. NIH3T3 cells did not support proliferation or survival (Fig. 4A). To study the requirement of direct adherence of TRL-01 to HESS-5, a membrane (BD cell culture insert) was inserted to prevent direct adherence between TRL-01 and HESS-5 but allow soluble factors to pass. The proliferation and survival of TRL-01 were significantly inhibited by the use of the cell culture insert ($n = 3$, $P < 0.01$; Fig. 4B). These results clearly indicate that TRL-01 required direct adherence to BM stroma cells for proliferation and survival.

To examine the effect of adherence to fibronectin on apoptosis, flow-cytometric analyses of TRL-01 cultivated on fibronectin-coated plates for 7 days were performed. A percentage of the apoptosis (lower-right fraction of two-color analyses using propidium iodide and annexin-V staining) were partly suppressed in the fibronectin-coated plates comparing to nontreated plates ($n = 3$, $P < 0.05$; Figs. 5A and 5B).

To determine the effect of growth factor on TRL-01 culture in a fibronectin-coated 6-well plate, 50 ng/mL of SCF, GM-CSF, G-SCF, TPO, or EPO was added. The cell numbers increased on treatment with GM-CSF ($n = 3$, $P < 0.01$), SCF ($n = 3$, $P < 0.01$), or G-CSF ($n = 3$, $P < 0.01$), whereas TPO and EPO had no effect on growth ($n = 3$; Fig. 6A). The survival of TRL-01 was slightly maintained under SCF ($n = 3$, $P < 0.05$) and G-CSF ($n = 3$, $P < 0.01$) treatment (Fig. 6B). No phenotypic or morphological changes were observed in TRL-01 cells treated with these factors ($n = 3$; data not shown).

To confirm the stroma dependency in vivo, we subcutaneously injected TRL-01 and HESS-5 into the dorsal regions of the NOG mice. Coinjection of TRL-01 and HESS-5 cells resulted in the tumors in the dorsal regions

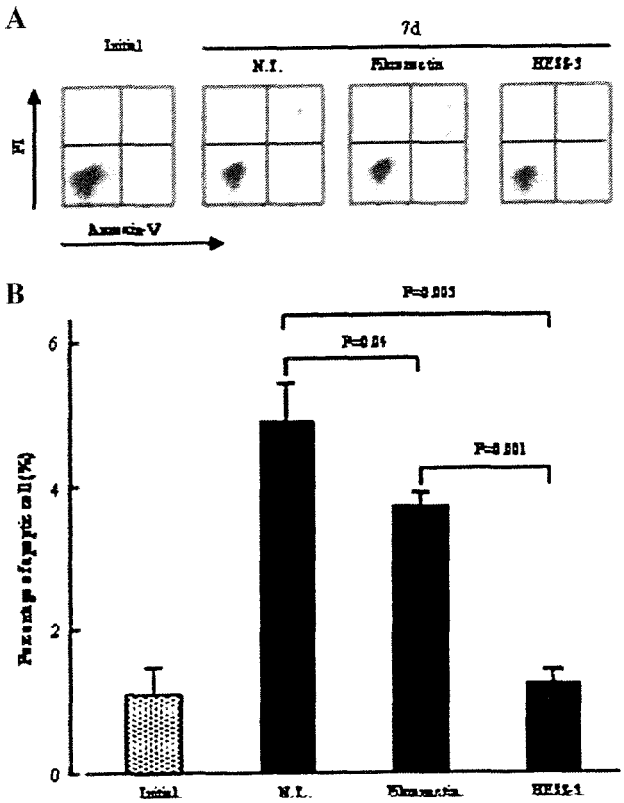

Fig. 5. Adhesion to the stroma cells inhibited apoptosis of TRL-01. (A) Flow-cytometric analyses of TRL-01 cells (1×10^5/mL, 5 mL), cultivated on fibronectin-coated 6-well plates or HESS-5 monolayer (5×10^3/mL) in 6-well plates for 7 days, with two-color propidium iodide and annexin-V staining. (B) Data indicate the percentage of the lower-right (apoptosis) fraction for 7 days cultivation of TRL-01. N.T., non-treated plate.

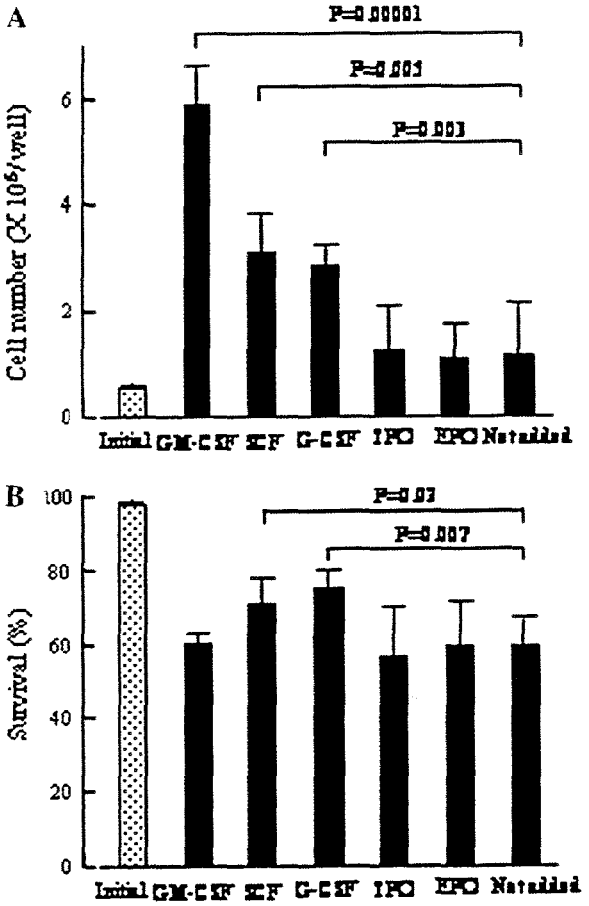

Fig. 6. Growth factors enhanced proliferation of TRL-01. TRL-01 (1×10^5/mL, 5 mL) cultivated on fibronectin-coated 6-well plates for 7 days with 50 ng/mL of growth factors. (A) Cell number. (B) Survival (%).

40 days after the injection ($n = 3$; Fig. 7A), whereas TRL-01 alone ($n = 3$) or HESS-5 alone ($n = 3$) did not form any tumors (Fig. 7A). In terms of pathology, the subcutaneous tumor was filled with myeloblastic cells ($n = 3$; Fig. 7B, plate 1) and was strongly stained with human CD45 immunostaining ($n = 3$; Fig. 7B, plate 2). Human $CD45^+$ cells were detected mainly in the BM and rarely found in other organs ($n = 3$; Fig. 7B, plates 3 and 4). From RT-PCR analysis, *MLL-ENL* expression was also confirmed in the subcutaneous tumor (Fig. 7C). These findings suggest that the proliferation and survival of TRL-01 depend on BM stroma cells in vivo as well as in vitro.

4. Discussion

One characteristic of TRL-01 is that it is an undifferentiated AML cell line with the *MLL-ENL* fusion gene. So far, several leukemia cell lines harboring *MLL-ENL* have been reported [11,18]. Their phenotypes are exclusively lymphoid, including pre-B ALL and pre-T ALL [19], although *MLL-ENL* is found in both myeloid and lymphoid lineages [20,21]. In most cases of *MLL-ENL*, generation of *MLL* exon 7 and *ENL* exon 2 chimeric transcripts was reported [11]. In the transcripts of TRL-01, exon 6 of the *MLL* gene was fused to exon 4 of the *ENL* gene. In both cases, an in-frame chimeric *MLL-ENL* is generated and major functional domains are the same (Fig. 3C).

Although the exact functional role of the MLL-ENL chimeric protein remains unclear, it has been suggested to be the upregulation of the transcription of *HOX9a* and *MEIS1*, which are associated with self-renewal and differentiation block [22]. It has recently been shown in a murine model that expression of *MLL-ENL* can convert a hematopoietic stem cell that has intrinsic self-renewal capacity, or even a committed hematopoietic progenitor cell that has no capacity for self-renewal, into a cell that has the properties of a leukemia stem cell [23]. Many investigators now think that a second hit such as a *FLT3* mutation would confer additional proliferative and survival advantages to these cells [24]. TRL-01, however, has neither surface expression nor

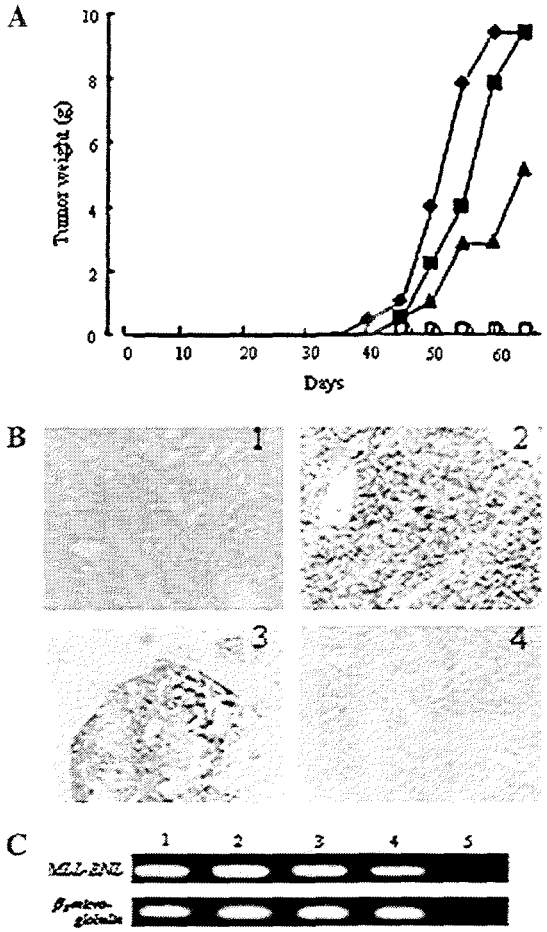

Fig. 7. TRL-01 required the coexistence of stroma cells for tumor formation in vivo. (A) Engraftment of BM MNC (2×10^6 cells) from the AML M0 leukemia patient and HESS-5 cells (6×10^4 cells) into dorsal regions of NOD/scid/γ_c^{null} (NOG) mice (close symbols, $n = 3$). As controls, either TRL-01 alone (squares; $n = 3$) or HESS-5 alone (triangles; $n = 3$) was similarly injected. Engrafted NOG mice were observed for 60 days. (B) Pathological findings of the subcutaneous tumor from NOG mice ($n = 3$) 60 days after the transplantation. The specimens from the subcutaneous tumor bearing NOG mice were sectioned and stained with H&E (panel 1, subcutaneous tumor) or developed human CD45 with DAB (panel 2, subcutaneous tumor; panel 3, bone marrow; panel 4, spleen). Original magnification: ×400. (C) RT-PCR of the *MLL-ENL* cDNA synthesized from the RNA in the subcutaneous tumor cells of NOG mice. Primers were *MLL* primer 4 and *ENL* primer 1, which gave PCR products at 438 bp. Lane 1, BM MNC at diagnosis; lane 2–4, cells collected from subcutaneous tumor of NOG mice ($n = 3$); lane 5, H_2O. As a positive control, primers for β_2-microglobulin were used.

mutation of *FLT3* (data not shown). Instead, the expression level of KIT/CD117 was high, although the *KIT* gene was not mutated (data not shown).

Another important characteristic of TRL-01 is the dependence on BM stroma cells in vivo and in vitro. Within 1 month after intravenous injection of TRL-01 into the tail, TRL-01 was exclusively found in the endosteal region of the BM and not in the other organs of mice. Subcutaneous injection of TRL-01 resulted in tumors only when HESS-5 was coinjected.

The HESS-5 stroma cell line has been used for ex vivo expansion of human hematopoietic progenitor cells, suggesting that HESS-5 cells have similar properties to human hematopoiesis-supporting cells in the BM [25,26]. HESS-5-conditioned medium was able to maintain the growth and viability of cells transiently. Soluble molecules produced by HESS-5 cells have been studied, and murine SCF, G-CSF, TPO, and nerve growth factor (NGF) are reported [26]. In the culture of TRL-01 without HESS-5, recombinant human SCF or GM-CSF promoted the proliferation of TRL-01 but did not maintain it. Given that murine SCF and GM-CSF do not cross-react with human receptors, these molecules are unlikely to have a key role in the proliferation of TRL-01.

Direct contact with HESS-5 was essential for the continuous survival of the cell line. Furthermore, proliferation of TRL-01 is also upregulated by direct contact with HESS-5 (data not shown). It is known that the fate of leukemia cells as well as hematopoietic stem cells (HSCs) is significantly affected by the adhesion mechanism [27]. Many adhesion molecules (such as integrin families, CD44, CD34, selectins, and immunoglobulin-like adhesion molecules) are present on the leukemia cell surface [28,29], although their roles are not fully understood. TRL-01 expresses VLA-4 and -5, and the apoptosis is partially blocked by the fibronectin-coated plate. Some studies also suggested that adhesion to fibronectin inhibited apoptosis of leukemia samples separated from the BM [30]. Accordingly, extracellular signaling via VLA-4 and -5 might be important for leukemia survival. Recent reports suggested that distinct intercellular interactions between the BM niche and HSCs are important for self-renewal, quiescence, and differentiation [31]. Leukemia cells may divide and survive in a similar way to HSCs.

Intravenously injected TRL-01 was located in the endosteal region of the NOG mouse after xenotransplantation. The mechanisms underlying the homing and lodging of TRL-01 in specific microenvironments is unknown. Currently, the chemokine SDF-1 and its receptor CXCR4 are known to play a critical role in the homing of normal hematopoietic progenitor cells to the BM [32,33]. TRL-01, however, does not express CXCR4 (data not shown). Furthermore, it remains unclear whether injected TRL-01 was localized to the murine BM endosteal region using the same mechanism by which it adheres to HESS-5. In our study, the coinjection of TRL-01 and HESS-5 resulted in a subcutaneous tumor in mice. HESS-5 might secrete a migration-inhibitory factor for TRL-01, which is different from SDF-1. Therefore, we believe that the self-organization of the tumor outside the BM might provide an interesting model to study homing of leukemia, leukemia-stroma interaction, angiogenesis, and drug development.

In conclusion, TRL-01 would be a useful cell line for studying not only the biology of *MLL-ENL* but also

the intercellular association between leukemia and the microenvironment.

Acknowledgments

This study was supported by grants-in-aid from the Ministry of Health and Welfare and from the Ministry of Education, Culture, Sports, Science and Technology, and was performed in cooperation with Research on the Human Genome, Tissue Engineering, Food Biotechnology from the Ministry of Health and Welfare. We thank Ms. Satomi Yamaji for technical assistance, and Ms. Manami Kira for secretarial assistance.

References

[1] Drexler HG, Matsuo AY, MacLeod RA. Continuous hematopoietic cell lines as model systems for leukemia-lymphoma research. Leuk Res 2000;24:881–911.

[2] Sen S, Zhou H, Andersson BS, Cork A, Freireich EJ, Stass SA. *p53* gene mutations with chromosome 17 abnormalities in chronic myelogenous leukemia blast crisis patients persist in long-term cell lines but may be acquired in acute myeloid leukemia cells in vitro. Cancer Genet Cytogenet 1995;82:35–40.

[3] Drexler HG. Review of alterations of the cyclin-dependent kinase inhibitor *INK4* family genes *p15*, *p16*, *p18* and *p19* in human leukemia-lymphoma cells. Leukemia 1998;12:845–59.

[4] Bonnet D, Dick JE. Human acute myeloid leukemia is organized as a hierarchy that originates from a primitive hematopoietic cell. Nat Med 1997;3:730–7.

[5] Reya T, Morrison SJ, Clarke MF, Weissman IL. Stem cells, cancer, and cancer stem cells. Nature 2001;414:105–11.

[6] Sell S. Stem cell origin of cancer and differentiation therapy. Crit Rev Oncol Hematol 2004;51:1–28.

[7] Ito M, Hiramatsu H, Kobayashi K, Suzue K, Kawahata M, Hioki K, Ueyama Y, Koyanagi Y, Sugamura K, Tsuji K, Heike T, Nakahata T. NOD/SCID/γ_c^{null} mouse: an excellent recipient mouse model for engraftment of human cells. Blood 2002;100:3175–82.

[8] Hiramatsu H, Nishikomori R, Heike T, Ito M, Kobayashi K, Katamura K, Nakahata T. Complete reconstitution of human lymphocytes from cord blood CD34+ cells using the NOD/SCID/γ_c^{null} mice model. Blood 2003;102:873–80.

[9] Ohbayashi K, Taniwaki M, Ninomiya M, Kiyoi H, Iida S, Ueda R, Naoe T. A xeno-transplantable plasma cell leukemia line with a split translocation of the *IgH* gene. Cancer Genet Cytogenet 2003;144:31–5.

[10] Ninomiya M, Kiyoi H, Ito M, Hirose Y, Ito M, Naoe T. Retinoic acid syndrome in NOD/scid mice induced by injecting an acute promyelocytic leukemia cell line. Leukemia 2004;18:442–8.

[11] Yamamoto K, Seto M, Iida S, Komatsu H, Kamada N, Kojima S, Kodera Y, Nakazawa S, Saito H, Takahashi T, Ueda R. A reverse transcriptase-polymerase chain reaction detects heterogeneous chimeric mRNAs in leukemias with 11q23 abnormalities. Blood 1994;83:2912–21.

[12] Thirman MJ, Levitan DA, Kobayashi H, Simon MC, Rowley JD. Cloning of *ELL*, a gene that fuses to *MLL* in a t(11;19)(q23;p13.1) in acute myeloid leukemia. Proc Natl Acad Sci U S A 1994;91:12110–4.

[13] Mitani K, Kanda Y, Ogawa S, Tanaka T, Inazawa J, Yazaki Y, Hirai H. Cloning of several species of *MLL/MEN* chimeric cDNAs in myeloid leukemia with t(11;19)(q23;p13.1) translocation. Blood 1995;85:2017–24.

[14] Megonigal MD, Rappaport EF, Wilson RB, Jones DH, Whitlock JA, Ortega JA, Slater DJ, Nowell PC, Felix CA. Panhandle PCR for cDNA: a rapid method for isolation of *MLL* fusion transcripts involving unknown partner genes. Proc Natl Acad Sci U S A 2000;97:9597–602.

[15] Raffini LJ, Slater DJ, Rappaport EF, Lo Nigro L, Cheung NK, Biegel JA, Nowell PC, Lange BJ, Felix CA. Panhandle and reverse-panhandle PCR enable cloning of der(11) and der(other) genomic breakpoint junctions of MLL translocations and identify complex translocation of *MLL*, *AF-4*, and *CDK6*. Proc Natl Acad Sci U S A 2002;99:4568–73.

[16] Kosugi H, Ito M, Yamamoto Y, Towatari M, Ito M, Ueda R, Saito H, Naoe T. In vivo effects of a histone deacetylase inhibitor, FK228, on human acute promyelocytic leukemia in NOD/Shi-scid/scid mice. Jpn J Cancer Res 2001;92:529–36.

[17] Tkachuk DC, Kohler S, Cleary ML. Involvement of a homolog of Drosophila trithorax by 11q23 chromosomal translocations in acute leukemias. Cell 1992;71:691–700.

[18] Drexler HG, Matsuo Y, MacLeod RA. Malignant hematopoietic cell lines: in vitro models for the study of erythroleukemia. Leuk Res 2004;28:1243–51.

[19] Rubnitz JE, Camitta BM, Mahmoud H, Raimondi SC, Carroll AJ, Borowitz MJ, Shuster JJ, Link MP, Pullen DJ, Downing JR, Behm FG, Pui CH. Childhood acute lymphoblastic leukemia with the *MLL-ENL* fusion and t(11;19)(q23;p13.3) translocation. J Clin Oncol 1999;17:191–6.

[20] Zeisig BB, Garcia-Cuellar MP, Winkler TH, Slany RK. The oncoprotein MLL-ENL disturbs hematopoietic lineage determination and transforms a biphenotypic lymphoid/myeloid cell. Oncogene 2003;22:1629–37.

[21] Daser A, Rabbitts TH. Extending the repertoire of the mixed-lineage leukemia gene *MLL* in leukemogenesis. Genes Dev 2004;18:965–74.

[22] Zeisig BB, Milne T, Garcia-Cuellar MP, Schreiner S, Martin ME, Fuchs U, Borkhardt A, Chanda SK, Walker J, Soden R, Hess JL, Slany RK. *Hoxa9* and *Meis1* are key targets for MLL-ENL-mediated cellular immortalization. Mol Cell Biol 2004;24:617–28.

[23] Cozzio A, Passegue E, Ayton PM, Karsunky H, Cleary ML, Weissman IL. Similar MLL-associated leukemias arising from self-renewing stem cells and short-lived myeloid progenitors. Genes Dev 2003;17:3029–35.

[24] Ono R, Nakajima H, Ozaki K, Kumagai H, Kawashima T, Taki T, Kitamura T, Hayashi Y, Nosaka T. Dimerization of MLL fusion proteins and FLT3 activation synergize to induce multiple-lineage leukemogenesis. J Clin Invest 2005;115:919–29.

[25] Shimakura Y, Kawada H, Ando K, Sato T, Nakamura Y, Tsuji T, Kato S, Hotta T. Murine stromal cell line HESS-5 maintains reconstituting ability of ex vivo-generated hematopoietic stem cells from human bone marrow and cytokine-mobilized peripheral blood. Stem Cells 2000;18:183–9.

[26] Tsuji T, Itoh K, Nishimura-Morita Y, Watanabe Y, Hirano D, Mori KJ, Yatsunami K. $CD34^{high+}$ $CD38^{low/-}$ cells generated in a xenogenic coculture system are capable of both long-term hematopoiesis and multiple differentiation. Leukemia 1999;13:1409–19.

[27] Hall BM, Gibson LF. Regulation of lymphoid and myeloid leukemic cell survival: role of stromal cell adhesion molecules. Leuk Lymphoma 2004;45:35–48.

[28] Bendall LJ, Kortlepel K, Gottlieb DJ. Human acute myeloid leukemia cells bind to bone marrow stroma via a combination of β-1 and β-2 integrin mechanisms. Blood 1993;82:3125–32.

[29] Gadhoum Z, Leibovitch MP, Qi J, Dumenil D, Durand L, Leibovitch S, Smadja-Joffe F. CD44: a new means to inhibit acute myeloid leukemia cell proliferation via $p27^{Kip1}$. Blood 2004;103:1059–68.

[30] Bendall LJ, Makrynikola V, Hutchinson A, Bianchi AC, Bradstock KF, Gottlieb DJ. Stem cell factor enhances the adhesion of AML cells to fibronectin and augments fibronectin-mediated anti-apoptotic and proliferative signals. Leukemia 1998;12:1375–82.

[31] Matsunaga T, Takemoto N, Sato T, Takimoto R, Tanaka I, Fujimi A, Akiyama T, Kuroda H, Kawano Y, Kobune M, Kato J, Hirayama Y, Sakamaki S, Kohda K, Miyake K, Niitsu Y. Interaction between leukemic-cell VLA-4 and stromal fibronectin is a decisive factor for minimal residual disease of acute myelogenous leukemia. Nat Med 2003;9:1158–65.

[32] Taichman RS. Blood and bone: two tissues whose fates are intertwined to create the hematopoietic stem-cell niche. Blood 2005;105:2631–9.

[33] Petit I, Goichberg P, Spiegel A, Peled A, Brodie C, Seger R, Nagler A, Alon R, Lapidot T. Atypical PKC-ζ regulates SDF-1-mediated migration and development of human $CD34^+$ progenitor cells. J Clin Invest 2005;115:168–76.

Available online at www.sciencedirect.com
SCIENCE DIRECT
ELSEVIER
Biochemical and Biophysical Research Communications 345 (2006) 1471–1480
BBRC
www.elsevier.com/locate/ybbrc

Histone deacetylase 3 (HDAC3) is recruited to target promoters by PML-RARα as a component of the N-CoR co-repressor complex to repress transcription *in vivo*

Akihide Atsumi [a,1], Akihiro Tomita [a,b,*,1], Hitoshi Kiyoi [b], Tomoki Naoe [a]

[a] *Department of Hematology, Nagoya University Graduate School of Medicine, Tsurumai-cho 65, Showa-ku, Nagoya 466-8560, Japan*
[b] *Department of Infectious Diseases, Nagoya University School of Medicine, Tsurumai-cho 65, Showa-ku, Nagoya 466-8560, Japan*

Received 18 April 2006
Available online 15 May 2006

Abstract

PML-RARα is a chimeric transcription factor tightly associated with acute promyelocytic leukemia. PML-RARα plays an important role in the aberrant transcription repression on the target genes of wild-type retinoic acid receptors. Here, we demonstrated that HDAC3, one component of the N-CoR transcription repressor complex, is a key regulator of the transcription repression by PML-RARα *in vivo*. Using immunoprecipitation, we demonstrated that PML-RARα interacts with N-CoR/HDAC3 *in vivo* without ligand. Next, using chromatin immunoprecipitation (ChIP) assay, this N-CoR/HDAC3 co-repressor complex was recruited to the endogenous target promoters (RARβ and CYP26) through PML-RARα. The neighboring histones were de-acetylated and gene expression was repressed. When HDAC3 protein was knocked down by RNA interference in PML-RARα-expressing cells, the endogenous target genes were significantly activated, which was also confirmed by promoter-luciferase reporter assay. These results provide evidence to show that the N-CoR/HDAC3 co-repressor complex is involved in the aberrant transcription regulation in PML-RARα-expressing cells.

Keywords: PML-RARα; N-CoR; HDAC3; Acute promyelocytic leukemia (APL); Transcription repression; Chromatin; SMRT

Transcription repression by the PML-RARα chimeric transcription factor plays an important role for the leukemogenesis in APL [1–3]. Recently, it has become widely recognized that all-*trans* retinoic acid (ATRA) is an excellent molecular targeting reagent for APL [4,5]. ATRA works directly on PML-RARα protein *in vivo*, and the aberrant transcription repression on many target genes can be released by administration of ATRA at the pharmacological concentration. Transcription de-repression on PML-RARα target genes is thought to be a key mechanism of the molecular targeting therapy and "transcription therapy" in APL.

Transcription repression by PML-RARα involves nuclear receptor co-repressor/silencing mediator for retinoid and thyroid hormone receptors (N-CoR/SMRT) co-repressor protein complexes that interact with PML-RARα in the absence of ligand [6]. N-CoR and SMRT are known to be key molecules for the transcription repression of nuclear receptors including retinoic acid receptor (RAR) and thyroid hormone receptor (TR) [7]. In the late 1990s, it had been reported that N-CoR/SMRT forms large protein complexes that contain other functional proteins including transcription co-repressors Sin3 and HDAC1 (histone deacetylase 1) [4,5,8,9]. In the last 5 years, numerous N-CoR/SMRT complexes other than Sin3/HDAC1 complex have been reported [10]. N-CoR/SMRT-TBL1/R1 (transducin beta like protein 1/related protein)-HDAC3 complex was purified from human nuclear extract by using a biochemical strategy [11–14]. N-CoR/SMRT-TBL1/R1-HDAC3 proteins exist in a large complex in human cells with an estimated size of 1.5–2 MDa. TBL1/R1, HDAC3, Kaiso [15], GPS2 [12] (G-protein pathway suppressor 2),

* Corresponding author. Fax: +81 52 744 2801.
E-mail address: atomita@med.nagoya-u.ac.jp (A. Tomita).
[1] These authors contributed equally to this work.

0006-291X/$ - see front matter © 2006 Elsevier Inc. All rights reserved.
doi:10.1016/j.bbrc.2006.05.047

and very recently JMJD2A [16] were identified as components of the N-CoR/SMRT complexes. TBL1/R1, which has WD40 repeats known to be a histone-binding motif, is critical for transcription repression [13,14,17,18]. Transcription repression introduced by these proteins is closely related to binding with de-acetylated histone on chromatin [19]. HDACs catalyze de-acetylation of specific lysine residues antagonizing histone acetyl transferases such as p300, PCAF, and GCN5 [20]. De-acetylation of histones in chromatin is closely related to transcription repression of target genes.

Nuclear receptor co-repressor null mice show abnormality in erythrocyte and thymocyte hematopoiesis [10], and disrupting N-CoR function using a dominant negative form expressed in immature leukemia cells induces cell differentiation [21]. Furthermore, interference of enzymatic activity of HDACs by administration of HDAC inhibitor, such as butyrate, trichostatin A (TSA), and valproic acid, induces differentiation in leukemia cells [22]. Taking these results into consideration, N-CoR-HDAC complexes are essential for hematopoiesis in development and are likely involved in cell differentiation in adult hematopoieses and pathogenesis in specific types of leukemia including APL. The determination of which N-CoR complex is utilized for the transcription regulation by PML-RARα is important for not only understanding of mechanisms of leukemogenesis, but also developing new molecular targeting therapies in APL. Here, we demonstrate directly *in vivo* that N-CoR-HDAC3 is recruited to endogenous target promoters through PML-RARα to repress PML-RARα target gene transcription. Our data indicate that N-CoR-HDAC3 complexes play an important role for the transcription repression in PML-RARα-expressing leukemic cells, and may be good candidates for molecular targets in the treatment of patients with APL.

Materials and methods

Cell culture. A human embryonic kidney cell line 293T cells was cultured in Dulbecco's modified Eagle's medium (DMEM) containing 10% fetal calf serum.

Plasmids. The coding sequence of PML-RARα was amplified by PCR and the Flag sequence was added in the forward primer as shown previously [17]. The PCR fragment was directly cloned into pcDNA4-His-Max-TOPO mammalian expression vector (Invitrogen, Carlsbad, CA). For the expression of short-hairpin RNA (shRNA) against HDAC3, pS65R-shHDAC3 that has CMV promoter for the expression of red fluorescent protein (RFP) was generated as follows. RFP sequence of pDsRed2-C1 (Stratagene, La Jolla, CA) was amplified using primers; RFP-forward 5′-GCCGCCACCGGTATGGCCTCCTCCGAGAAC-3′, reverse 5′-GC CGCCAGATCTTCACAGGAACAGGTGGTGGCG-3′. After digestion by *Age*I and *Bgl*II, the RFP fragment was inserted into *Age*I–*Bgl*II sites of pS65T-C1 vector (Stratagene). Short-hairpin RNA sequence with H1 promoter from shRNA expression vector p*Silencer* 3.0-H1 (Ambion, Austin, TX) was amplified by PCR using the following primers; shH1-forward 5′-GCCGCCCTTAAGGATATCTTCCCAGTCACGACGTT GTA-3′, reverse 5′-GCCGCCCTTAAGGATATCCACAGGAAACAGC TATGACC-3′. This fragment was inserted into *Afl*II site after blunting (pS65R-siH1). For shRNA sequence for HDAC3, two oligos (forward 5′-GATCCGATGCTGAACCATGCACCTTTCAAGAGAAGGTGCA TGGTTCAGCATCTTTTTTGGAAA-3′, reverse 5′-AGCTTTTCCAA AAAAGATGCTGAACCATGCACCTTCTCTTGAAAGGTGCATG GTTCAGCATCG-3′) generated by Nippon Gene Laboratory (Sendai, Japan) were annealed and inserted into *Bam*HI–*Hin*dIII sites of pS65R-shH1 (pS65R-shHDAC3). The sequence for the siHDAC3 and its specificity were published previously [31]. RARβ and CYP26 promoter sequences were amplified by PCR using genomic DNA obtained from the author's white blood cells. PCR primers were designed based on the genomic DNA sequences from GenBank (RARβ; X56849, CYP26; AL358613), and the primer sequences are; RARβ-pro-forward 5′-GCCG CCGGTACCCCAGAACACACAGCTGGTAA-3′, reverse 5′-GCCGC CAAGCTTGATCTCCCTTGCACTGAATG-3′, CYP26-pro-forward 5′-GCCGCCAAGCTTGTACAGATGGAGCCGGGCTC-3′, reverse 5′-GCCGCCAAGCTTGGCGCGCCGCGACCTCCCG-3′. These primers amplify the promoter sequences just before the translation start codon (ATG), and the lengths of those fragments are 1313 and 1000 bp, respectively. Those fragments were cut by *Kpn*I and *Hin*dIII, and inserted into the *Kpn*I–*Hin*dIII sites of pGL2-basic luciferase reporter vector (Promega).

RNA extraction and RT-PCR. Total RNA was isolated from 293T cells and complementary DNA was obtained by using SuperScriptII reverse transcriptase (Invitrogen). PCR was carried out as follows; 95 °C 3 min 1 cycle, 94 °C 30 s–55 °C 30 s–72 °C 40 s 25 to 30 cycles for semi-quantitative PCR. PCR primers for the cording sequences of RARβ, CYP26, and HDAC3 are as follows; RARβ-forward 5′-ATGTTTGACTGTATGG ATGTTC-3′, reverse 5′-CCCACTTCAAAGCACTTCTG-3′, CYP26-forward 5′-GATGAAGCGCAGGAAATACG-3′ and reverse 5′-ATGGC GATTCGGAACATGAG-3′, HDAC3-forward 5′-CTGGCTTCTGCTA TGTCAAC-3′, HDAC3-reverse 5′-ACATATTCAACGCATTCCCCA-3′, HDAC1-forward 5′-GAGATGACCAATACCACAG-3′, HDAC1-reverse 5′-TATCCCGTAGGTCCCCAGT-3′. As an internal control, β-actin primers were used, β-actin-forward 5′-TCACTCATGAAGATCC TCA-3′, reverse 5′-TTCGTGGATGCCACAGGAC-3′.

Quantitative RT-PCR. Quantitative PCR (TaqMan real-time PCR) was performed using ABI Prism 7000 (Applied Biosystems). Probes and primers for RARβ (Hu00233507) and CYP26 (Hs00175627) were purchased from Applied Biosystems. As an internal control, endogenous GAPDH mRNA was measured (Hu GAPDH).

Antibodies. Affinity purification of N-CoR antiserum was described previously [17]. Anti-human HDAC3, HDAC1, and Sin3 were purchased from Abcam (Cambridge, UK). Acetylated histone H4 antibody was purchased from Upstate (Waltham, MA). Anti-Flag antibody was purchased from Sigma (St. Louis, MO).

Immunoprecipitation (IP) and immunoblotting. Flag-tagged PML-RARα expression vector (2 μg) was transfected into 293T cells (5×10^5) using FuGene6 (Roche). After 2 days of incubation, cells were lysed in 400 μl lysis buffer (50 mM Tris–HCl, pH 8.0, 1.5 mM $MgCl_2$, 1 mM EGTA, 5 mM KCl, 10% glycerol, 0.5% NP-40, 300 mM NaCl, 0.2 mM PMSF, 1 mM DTT, and Complete-mini protease inhibitor tablet (Roche)). After centrifugation, the supernatant was put into a new tube, to which was added 400 μl of dilution buffer (50 mM Tris–HCl, pH 8.0, 1.5 mM $MgCl_2$, 1 mM EGTA, 5 mM KCl, 10% glycerol, 0.2 mM PMSF, 1 mM DTT, and protease inhibitor tablet). IP was performed using Flag-M2 affinity beads (Sigma) as indicated previously [18,23]. After IP, agarose beads were washed three times in wash buffer (50 mM Tris–HCl, pH 8.0, 1.5 mM $MgCl_2$, 1 mM EGTA, 5 mM KCl, 10% glycerol, 0.05% NP-40, 150 mM NaCl, 0.2 mM PMSF, 1 mM DTT, and protease inhibitor tablet), and the purified protein was eluted with 100 mM glycine. Eluted proteins were analyzed by immunoblotting using specific antibodies.

Chromatin immunoprecipitation (ChIP) assay. Chromatin immunoprecipitation assay was performed using 293T cells (1×10^6 cells for one assay) as indicated on the manufacturer's instruction manual (Upstate) and previous report [17]. Wash buffers I to IV were prepared as follows; ChIP I (0.1% sodium deoxycholate, 1% Triton X-100, 2 mM EDTA, 20 mM Tris–HCl, pH 8.0, and 150 mM NaCl), ChIP II (0.1% sodium deoxycholate, 1% Triton X-100, 2 mM EDTA, 20 mM Tris–HCl, pH 8.0, and 500 mM NaCl), ChIP III (0.25 M LiCl, 0.5% NP-40, 0.5% sodium deoxycholate, 1 mM EDTA, and 10 mM Tris–HCl, pH 8.0), ChIP IV

(10 mM Tris–HCl, pH 8.0, and 1 mM EDTA). All washing buffers contain 0.2 mM PMSF, 1 mM DTT, and protease inhibitor tablet (Roche). After washing and reverse-crosslinking, immunoprecipitated DNA was purified and PCR was performed. The following PCR primers were used to detect the immunoprecipitated promoter DNA; RARβ promoter forward 5′-TCCTGGCTGTCTGCTTTTGT-3′, reverse 5′-CAAAAAGCCTTCC GAATGCG-3′, CYP26 promoter forward 5′-TAAAGATTTTGGGCA GCGCC-3′, reverse 5′-CATCTGCAAGGTTTCCCCAA-3′, RARβ gene 3′ region forward 5′-CCCTGGTTATCTGTCATAGC-3′, reverse 5′-ACT GAAGGTACTGGGGAATG-3′, and CYP26 gene 3′ region forward 5′-GGGGTTTCAGTGCTTTTTGC-3′, reverse 5′-CAATGCTGGAAA CCTGGC-3′.

Luciferase reporter assay. 293T cells (5×10^4 cells/one assay) were plated in 12-well plates and incubated for one day. Then, pS65R-shH1 or pS65R-shHDAC3 (concentration is indicated in legends) were transfected. Twenty-four hours after the first transfection, pcDNA4-F-PML-RAR (0.5 μg) and luciferase reporter plasmids RARβ-Luc or CYP26-Luc (1 μg) were transfected. Cells were incubated for 2 days with or without 1 μM ATRA and lysed for luciferase assay. Dual-luciferase assay kit (Promega) was used for this assay, and chemoluminescence signal was measured by Luminometer AB-2250 (ATTO, Tokyo, Japan).

Results

PML-RARα interacts with N-CoR and HDAC3 in the absence of ligand

To determine whether N-CoR-HDAC3 complexes are involved in the transcription regulation of PML-RARα *in vivo*, we first tried to co-IP complex components from 293T cells (Fig. 1). The expression vector for Flag-tagged PML-RARα (F-PML-RAR) was transiently overexpressed in 293T cells and incubated at 37 °C with (lanes 2–4 and 7–9) or without ATRA (lanes 1, 5, 6, and 10). Two days after transfection, IP using Flag-M2 affinity beads was performed on whole cell lysate. Each eluted protein sample was immunoblotted using affinity purified rabbit anti-N-CoR antiserum [17] and rabbit anti-HDAC3 antibody (Abcam). F-PML-RAR interacts with endogenous N-CoR and HDAC3 in the absence of ATRA (lane 6). In the presence of ATRA, N-CoR and HDAC3 were dissociated from F-PML-RAR in a dose-dependent manner (lanes 7–9). We also tried to detect F-PML-RAR interacting with endogenous HDAC1 and Sin3, which were reported to be components of N-CoR co-repressor complexes [24]. In this assay system, we could not detect endogenous Sin3-HDAC1 interaction with F-PML-RAR (lanes 6–10). Longer exposure failed to detect Sin3-HDAC3 interaction with F-PML-RAR (data not shown). Expression levels of endogenous N-CoR, HDAC3, HDAC1, Sin3, and exogenous F-PML-RAR are indicated in lanes 1–5 (Pre-IP). Almost the same amount of those proteins was expressed with or without ATRA. These data indicate that endogenous N-CoR-HDAC3 interacts with PML-RARα without ligand, and the affinity of those interactions is strictly regulated by ATRA.

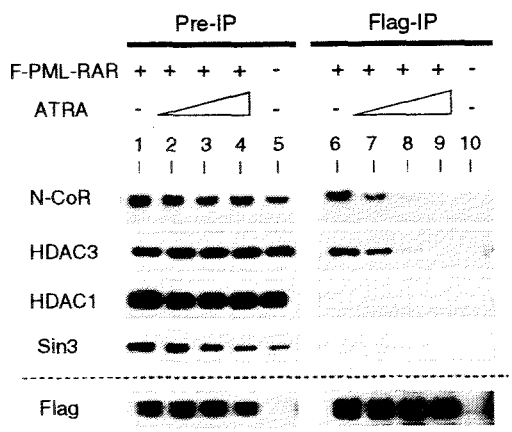

Fig. 1. Endogenous HDAC3 and N-CoR interact with PML-RARα in the absence of ligand. Flag-tagged-PML-RARα (F-PML-RAR) was transiently overexpressed in 293T cells and incubated for 2 days. Different concentrations of ATRA (lane 2, 10 nM; lane 3, 100 nM; lane 4, 1 μM) were added during incubation. Cells were lysed and subjected to immunoprecipitation using Flag-M2 affinity beads. Cell lysate (pre-IP) and IP (Flag-IP) samples were used for Western blotting. Detection was performed using anti-Flag, N-CoR, HDAC3, HDAC1, and Sin3 antibodies. Note that N-CoR/HDAC3 dissociated from F-PML-RAR in the presence of ATRA (lane 9). F-PML-RAR was successfully immunoprecipitated by Flag affinity beads (Flag; lanes 6–9).

Exogenous PML-RARα regulates target gene expression in vivo

To determine whether the overexpressed F-PML-RAR chimeric protein is functional *in vivo*, we analyzed RARα target gene expression by RT-PCR using 293T cells. Two RARα target genes [25], RARβ and CYP26, were selected for this assay. F-PML-RAR was overexpressed in 293T cells and incubated for 1 day with or without increasing amounts of ATRA as indicated in Fig. 2A. Total RNA was purified and RT-PCR using RARβ, CYP26, and β-actin specific primers were performed. These primers were designed for the coding sequences that are located on different exons to eliminate amplifying genomic DNA contamination in the PCRs. As shown in Fig. 2A, endogenous RARβ and CYP26 mRNA expression is significantly repressed in the presence of F-PML-RAR (lane 2 vs. lane 1). In contrast, RARβ and CYP26 expression is induced by ATRA in a dose-dependent manner (lanes 3–5). To compare the expression level in each sample, quantitative PCR (real-time PCR) was performed (Fig. 2B). The same cDNA samples in Fig. 2A were used for this assay. Repressed expression of RARβ and CYP26 by PML-RARα (lanes 2, adjusted as 1) was significantly relieved as ATRA concentration increased. These data indicate that exogenous F-PML-RAR in 293T cells regulates endogenous RARα target gene expression. F-PML-RAR works as repressor in the absence of ligand and as an activator with ligand.

Endogenous N-CoR-HDAC3 is recruited to PML-RARα target gene promoters in the absence of ligand

Next, we performed ChIP assay in 293T cells to show recruitment of N-CoR-HDAC3 complexes to target gene